

# Neutral and Cationic [Bis( $\eta^1$ -amidosilyl)- $\eta^5$ -cyclopentadienyl]titanium and -zirconium Complexes: Synthesis, X-ray Molecular Structures and DFT Calculations

Jesús Cano,<sup>[a]</sup> Pascual Royo,\*<sup>[a]</sup> Heiko Jacobsen,<sup>[b][‡]</sup> Olivier Blacque,<sup>[b]</sup> Heinz Berke,<sup>[b]</sup> and Eberhardt Herdtweck<sup>[c]</sup>

**Keywords:** Cations / Cyclopentadienyl ligands / Density functional calculations / Nitrogen ligands / Titanium / Zirconium

Treatment of  $\text{LiNHtBu}$  with THF solutions of  $\text{C}_5\text{H}_4(\text{SiMe}_2\text{Cl})_2$  gave  $\text{C}_5\text{H}_4(\text{SiMe}_2\text{NHtBu})_2$  (**1**). Deprotonation of **1** with  $\text{M}(\text{NMe}_2)_4$  ( $\text{M} = \text{Ti}, \text{Zr}$ ) under different conditions provided the monocyclopentadienyl complexes  $[\text{M}\{\eta^5\text{-C}_5\text{H}_3\text{-}[\text{SiMe}_2(\text{NHtBu})_2]\}(\text{NMe}_2)_3]$  [ $\text{M} = \text{Ti}$  (**2**),  $\text{Zr}$  (**3**)] and the single ( $\eta$ -amidosilyl)cyclopentadienyl compounds  $[\text{M}\{\eta^5\text{-C}_5\text{H}_3\text{[SiMe}_2(\text{NHtBu})]\}[\text{SiMe}_2(\eta^1\text{-NHtBu})](\text{NMe}_2)_2]$  [ $\text{M} = \text{Ti}$  (**4**),  $\text{Zr}$  (**5**)]. The related dibenzyl compounds  $[\text{M}\{\eta^5\text{-C}_5\text{H}_3\text{[SiMe}_2(\text{NHtBu})]\}[\text{SiMe}_2(\eta^1\text{-NHtBu})](\text{CH}_2\text{Ph})_2]$  [ $\text{M} = \text{Ti}$  (**6**),  $\text{Zr}$  (**7**)] resulted from treatment of **1** with  $\text{M}(\text{CH}_2\text{C}_6\text{H}_5)_4$  ( $\text{M} = \text{Ti}, \text{Zr}$ ). Further deprotonation of the amido complexes **4** and **5** and the benzyl complexes **6** and **7** by heating in toluene solution gave the bis( $\eta$ -amidosilyl)cyclopentadienyl complexes

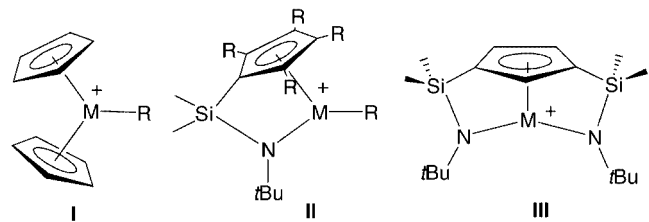
$[\text{M}\{\eta^5\text{-C}_5\text{H}_3\text{[SiMe}_2(\eta^1\text{-NHtBu})]\}_2](\text{NMe}_2)$  [ $\text{M} = \text{Ti}$  (**8**),  $\text{Zr}$  (**9**)] and  $[\text{M}\{\eta^5\text{-C}_5\text{H}_3\text{[SiMe}_2(\eta^1\text{-NHtBu})]\}_2](\text{CH}_2\text{Ph})$  [ $\text{M} = \text{Ti}$  (**10**),  $\text{Zr}$  (**11**)], respectively. Treatment of the monobenzyl complexes **10** and **11** with  $\text{B}(\text{C}_6\text{F}_5)_3$  yielded the cationic compounds  $[\text{M}\{\eta^5\text{-C}_5\text{H}_3\text{[SiMe}_2(\eta^1\text{-NHtBu})]\}_2]^+$  as  $[(\text{CH}_2\text{Ph})\text{B}(\text{C}_6\text{F}_5)_3]^-$  [ $\text{M} = \text{Ti}$  (**12**),  $\text{Zr}$  (**13**)] salts. All new compounds were characterized by NMR spectroscopy, and the crystal structures of **10** and **13** were studied by diffraction methods. DFT calculations for the neutral and cationic species are described and provide an explanation for the unusual  $\eta^1$  coordination of a phenyl ring to a group-4 metal cation.

(© Wiley-VCH Verlag GmbH & Co. KGaA, 69451 Weinheim, Germany, 2003)

## Introduction

The group-4 metallocenes  $[\text{MCp}_2\text{X}_2]$ <sup>[1]</sup> and cyclopentadienylamido complexes  $[\text{M}(\eta^5\text{-C}_5\text{R}_4\text{-E-}\eta^1\text{-NR}')\text{X}_2]$ <sup>[2]</sup> are the two essential types of catalyst precursors for insertion polymerization of olefins based on the use of cyclopentadienyl ligands. After alkyl abstraction by a Lewis acid {MAO,  $\text{B}(\text{C}_6\text{F}_5)_3$ ,  $[\text{CPh}_3]\text{B}(\text{C}_6\text{F}_5)_4$ } the metallocene compounds generate the cationic, coordinatively unsaturated, 14-electron  $d^0$   $[\text{MCp}_2\text{R}]^+$  species,<sup>[3]</sup> whereas the cyclopentadienylamido complexes provide the electronically more unsaturated 12-electron  $d^0$   $[\text{M}(\eta^5\text{-C}_5\text{R}_4\text{-E-}\eta^1\text{-NR}')\text{R}']^+$  cations.<sup>[4]</sup>

The technological applications<sup>[5]</sup> of these “constrained-geometry” catalysts are based not only on their electronic unsaturation, but also on their sterically open reactive sites, combined with rigidity of the molecular framework and thermal stability. These features facilitate the coordination of bulkier olefins, allowing the synthesis of various copolymers of ethylene with 1-hexene, 1-octene, styrene and other larger olefins.



Scheme 1. Types of metallocene and (cyclopentadienylsilyl)amido cations

Amido ligands are  $\pi$ -donors and in this respect resemble Cp ligands. Even if  $\pi$ -electrons are included, however, the formal electron count of a single group never reaches that of the Cp moiety. Replacement of one Cp by an amido group, as demonstrated in structures **I** and **II**, establishes a 12-electron cyclopentadienylamido complex<sup>[6]</sup> on the basis

[a] Departamento de Química Inorgánica, Facultad de Química, Universidad de Alcalá, Campus Universitario, 28871 Alcalá de Henares, Spain  
Fax: (internat.) + 34-91/8854683  
E-mail: pascual.royo@uah.es

[b] Anorganisch-chemisches Institut der Universität Zürich Winterthurerstrasse 190, 8057 Zürich, Switzerland  
Fax: (internat.) + 41-1/635-6802  
E-mail: hberke@aci.unizh.ch

[c] Anorganisch-chemisches Institut der Technischen Universität München Lichtenbergstrasse 4, 85747 Garching bei München, Germany

[‡] Present address: KemKom, 1864 Burfield Ave., Ottawa, Ontario K1J 6T1, Canada, E-mail: jacobsen@kemkom.com

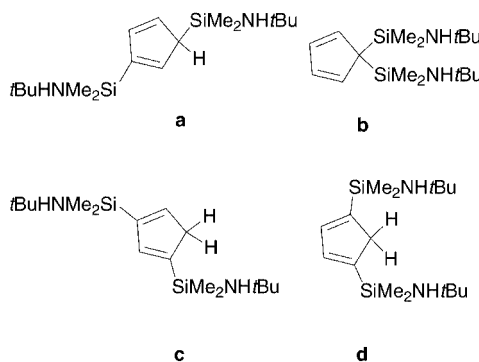
Supporting information for this article is available on the WWW under <http://www.eurjic.org> or from the author.

of a 14-electron metallocene species **I**. Structures of type **III** with two amido ligands would indeed have the formal electron count of **I**. Despite this, complexes **III** are special, since they do not bear an alkyl group ready for Ziegler–Natta-type insertion polymerizations. Nevertheless, we have reported<sup>[7]</sup> that they still have potential for polarized metal–olefin binding similar to, for instance, the 18-electron  $\text{Cp}_3\text{M}^+$  series ( $\text{M} = \text{Ti}, \text{Zr}$ ).<sup>[8]</sup> For this reason we decided to study the synthesis and chemical behaviour of [bis(amidosilyl)cyclopentadienyl]titanium and -zirconium complexes of type **III**.

Here we report the syntheses of monocyclopentadienyl  $[\text{M}\{\eta^5-\text{C}_5\text{H}_3[\text{SiMe}_2(\text{NH}t\text{Bu})_2]\}_2\text{X}_3]$ , (amidosilyl)cyclopentadienyl  $[\text{M}\{\eta^5-\text{C}_5\text{H}_3[\text{SiMe}_2(\text{NH}t\text{Bu})][\text{SiMe}_2(\eta^1-\text{N}t\text{Bu})]\}\text{X}_2]$  and bis(amidosilyl)cyclopentadienyl  $[\text{M}\{\eta^5-\text{C}_5\text{H}_3(\text{SiMe}_2-\eta^1-\text{N}t\text{Bu})_2\}\text{X}]$  group-4 metal compounds and their cationic  $[\text{M}\{\eta^5-\text{C}_5\text{H}_3(\text{SiMe}_2-\eta^1-\text{N}t\text{Bu})_2\}]^+$  derivatives. The X-ray molecular structures of the neutral  $[\text{Ti}\{\eta^5-\text{C}_5\text{H}_3[\text{SiMe}_2(\eta^1-\text{N}t\text{Bu})_2]\}(\text{CH}_2\text{Ph})]$  and the cationic  $[\text{Zr}\{\eta^5-\text{C}_5\text{H}_3[\text{SiMe}_2(\eta^1-\text{N}t\text{Bu})_2]\}^+](\text{CH}_2\text{C}_6\text{H}_5)\text{B}(\text{C}_6\text{F}_5)_3^-$  complexes were determined by diffraction methods and DFT calculations were carried out for the neutral and cationic species.

## Results and Discussion

The cyclopentadiene  $\text{C}_5\text{H}_4(\text{SiMe}_2\text{NH}t\text{Bu})_2$  (**1**) was isolated as a yellow liquid by treatment of the reported bis(chlorosilyl)cyclopentadiene<sup>[9]</sup> with 2 equiv. of  $\text{LiNH}t\text{Bu}$  in THF and was characterized by  $^1\text{H}$  and  $^{13}\text{C}$  NMR spectroscopy as a mixture of isomers (Scheme 2). The  $^1\text{H}$  NMR spectrum of **1** recorded at 20 °C indicated a mixture of isomers **a**, **b**, **c** and **d** in a molar ratio of 8:4:1.3:1.



Scheme 2. Isomers of  $\text{C}_5\text{H}_4(\text{SiMe}_2\text{NH}t\text{Bu})_2$  observed by NMR spectroscopy

In comparison with other previously reported disilyl-substituted compounds  $\text{C}_5\text{H}_4(\text{SiR}_3)_2$ ,<sup>[10]</sup> in which the 1,1-isomer (**b**;  $\text{R} = \text{Me}, \text{Cl}$ ) is by far the major component, the steric hindrance caused by the bulkier substituents ( $\text{R} = \text{NH}t\text{Bu}$ ) means that the 1,3-isomer (**a**; two broad  $\text{SiMe}_2$  singlets) is the major component in the isomeric mixture of **1**, being more favourable than the 1,1-isomer (**b**; one broad  $\text{SiMe}_2$  singlet), as shown in Scheme 2. The other two isomers (2,4- and 2,5-), with both silyl groups bound to  $\text{sp}^2$  carbon atoms, were less abundant components. All of these

isomers interconvert, probably through successive 1,2-shifts of the silyl groups,<sup>[10]</sup> and increasing temperatures increase the **a/b** ratio to 4:1 at 50 °C, 8:1 at 70 °C and more than 10:1 at temperatures higher than 80 °C. The broad signals observed for **1a** at 20 °C appeared as four singlets when the  $^1\text{H}$  NMR spectrum was recorded at –40 °C.

The tetraamide  $\text{M}(\text{NMe}_2)_4$ <sup>[11]</sup> and tetrabenzyl  $\text{M}(\text{CH}_2\text{Ph})_4$ <sup>[12]</sup> compounds ( $\text{M} = \text{Ti}, \text{Zr}$ ) were used to deprotonate the cyclopentadiene compound **1**, which possesses three acidic protons, to generate the metal-coordinated cyclopentadienyl ligand.

### Monocyclopentadienyl Compounds

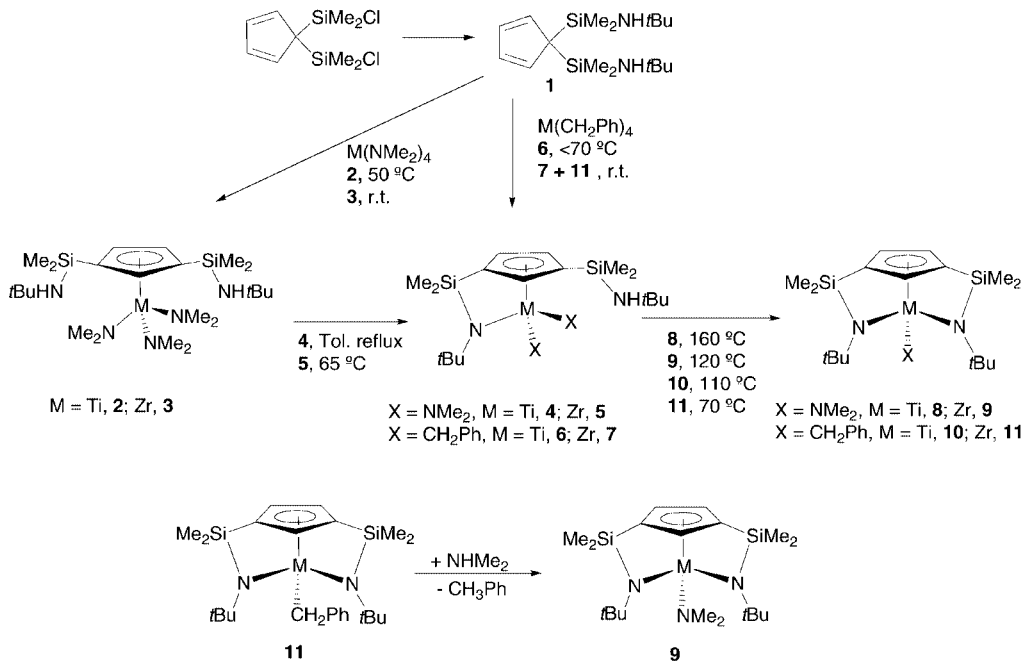
Immediate deprotonation of the most acidic cyclopentadiene proton took place when a toluene solution of **1** was treated at room temperature with 1 equiv. of  $\text{Zr}(\text{NMe}_2)_4$  to give the monocyclopentadienyl compound **3** (Scheme 3) as the unique reaction product after 1 h (100% NMR yield). When  $\text{Ti}(\text{NMe}_2)_4$  was used, heating at 50 °C was required to complete the reaction, the analogous titanium derivative **2** being isolated. Compound **2** was isolated as a dark red oil in quantitative yield after removal of the toluene and extraction into hexanes. The related tribenzyltitanium and -zirconium derivatives could not be isolated when  $\text{M}(\text{CH}_2\text{Ph})_4$  was used<sup>[13]</sup> because further deprotonation to give the mono- and bis(silylamido) benzyl derivatives took place very easily at room temperature.

The different thermal conditions required to deprotonate the tribasic diaminocyclopentadiene **1** show that the deprotonation with irreversible toluene elimination by the tetrabenzyl compounds  $\text{M}(\text{CH}_2\text{Ph})_4$  is much easier than the reversible elimination of amine by the amido derivatives  $\text{M}(\text{NMe}_2)_4$ , and that the zirconium compounds are more easily deprotonated than the more crowded titanium analogues, in spite of their weaker Ti–C and Ti–N bonds.<sup>[14]</sup> In all reactions the first deprotonation involves the most acidic cyclopentadiene proton.

The  $^1\text{H}$  NMR spectra of **2** and **3** in  $\text{C}_6\text{D}_6$  each show equivalent silylamido groups with NH ( $\delta = 1.04, 1.08 \text{ ppm}$ ),  $t\text{Bu}$  ( $\delta = 1.16, 1.15 \text{ ppm}$ ), and diastereotopic  $\text{SiMe}_2$  ( $\delta = 0.41, 0.43 \text{ ppm}$ ;  $\delta = 0.42, 0.44 \text{ ppm}$ ) resonances close to those observed for **1**. Additionally, they each show an  $A_2\text{B}$  spin system for the ring protons and one singlet for all three equivalent  $\text{NMe}_2$  groups. The expected spectral features were also observed in the  $^{13}\text{C}$  NMR spectra, which each show one downfield shifted ring  $C_{ipso}$  resonance ( $\delta = 127.8, 127.2 \text{ ppm}$ ) and  $\Delta\delta$  ( $\delta_{\text{C}_{tert}} - \delta_{\text{C}_{Me}}$ ) values<sup>[15]</sup> (15.3 ppm and 15.4 ppm) consistent with the presence of uncoordinated  $\text{SiMe}_2-\text{NH}t\text{Bu}$  groups.

### Single (Amidosilyl)cyclopentadienyl Compounds

When toluene or THF solutions of complex **3**, prepared at room temperature, were heated at 65 °C, complete transformation of **3** into **5** was observed after 3 h. Compound **5** was the only NMR-detectable product under these conditions, and it could be isolated as a brown solid and characterized by elemental analysis and NMR spec-



Scheme 3. Synthesis of cyclopentadienyl- and [(amidosilyl)- and bis(amidosilyl)cyclopentadienyl]titanium and -zirconium amide and benzyl complexes

troscopy. A similar transformation of **2** was achieved when a toluene solution of previously isolated **2** was heated at reflux for 5 h. The deprotonation of only one of the SiMe<sub>2</sub>N*t*Bu substituents with elimination of amine NHMe<sub>2</sub> occurred in a selective way to give pure **4**, which was isolated as a dark red oil and characterized by elemental analysis and NMR spectroscopy.

The related dibenzyl[*ansa*-(cyclopentadienylsilyl)amido]-titanium compound **6** was produced when a toluene solution of **1** and Ti(CH<sub>2</sub>Ph)<sub>4</sub> was heated (below 70 °C) for 5 h. Higher temperatures could not be used, since further deprotonation would then occur, yielding small amounts of **8**. Under these conditions, **6** was the only reaction product that could be isolated, as a red-brown solid, and identified by elemental analysis and NMR spectroscopy. The third deprotonation could not be avoided when Zr(CH<sub>2</sub>Ph)<sub>4</sub> was used, because deprotonation then occurs even at low temperature to give a mixture of **7** and other minor components. Because the products could not be separated, **7** was only characterized by NMR spectroscopy.

Coordination of the  $\eta^5$ -cyclopentadienyl ligand increases the acidity of the NH*t*Bu amino protons [ $\delta$  = 1.04 (**2**), 1.08 (**3**) ppm], and this is further increased after abstraction of the first amino hydrogen atom [ $\delta$  = 0.86 (**4**), 0.85 (**5**) ppm]. For these reasons the reactions with the titanium reagents could be carried out selectively to give pure amido and benzyl compounds, whereas the tribenzyl compounds could not be isolated at room temperature.

The <sup>1</sup>H NMR spectra of the silylamido compounds **4–7** in C<sub>6</sub>D<sub>6</sub> each show an ABC spin system for the three ring protons while the <sup>13</sup>C NMR spectra exhibit five resonances for the inequivalent ring carbon atoms, as expected for asymmetric molecules. Four resonances (<sup>1</sup>H and <sup>13</sup>C) for

the SiMe<sub>2</sub> moieties and two for the *t*Bu groups (<sup>1</sup>H and <sup>13</sup>C), along with two <sup>13</sup>C resonances for their quaternary carbon atoms, are also observed for the two non-equivalent SiMe<sub>2</sub>N*t*Bu and SiMe<sub>2</sub>NH*t*Bu groups. Both can be easily distinguished by the different  $\Delta\delta$  values<sup>[15]</sup> observed in the <sup>13</sup>C NMR spectra, which are smaller [15.5 (**4**), 15.7 (**5**), 16.0 (**6**, **7**) ppm] for uncoordinated NH*t*Bu groups than for bridging N*t*Bu groups [26.4 (**4**), 21.7 (**5**), 27.3 (**6**), 23.7 (**7**) ppm]. The amido complexes **4** and **5** also show two signals (<sup>1</sup>H and <sup>13</sup>C) for non-equivalent NMe<sub>2</sub> ligands, whereas the benzyl derivatives **6** and **7** show four <sup>1</sup>H doublets and two <sup>13</sup>C resonances for diastereotopic methylene protons and carbon atoms of two non-equivalent benzyl ligands.

The chemical shifts observed in the <sup>1</sup>H and <sup>13</sup>C NMR spectra for all of the ring substituents of the analogous titanium and zirconium complexes show very slight differences, whereas resonances for the additional NMe<sub>2</sub> and CH<sub>2</sub>Ph ligands appear at a lower field for the titanium than for the zirconium analogues. The *tert*-butyl <sup>1</sup>H and <sup>13</sup>C resonances of the coordinated amido ligand are shifted down-field with respect to a free NH*t*Bu group as a consequence of the  $\pi$ -donation to the metal centre, which is also consistent with a higher value of  $\Delta\delta$ .

#### Bis(amidosilyl)cyclopentadienyl Compounds

Complete deprotonation of the uncoordinated SiMe<sub>2</sub>–NH*t*Bu groups in the dibenzyl complexes **6** and **7** required heating of their toluene solutions under reflux or at 70 °C, respectively, to give the bis(silylamido) compounds **10**, isolated as orange crystals and **11**, isolated as a brown solid. Both complexes were identified by elemental analyses and NMR spectroscopy. Temperatures higher than reflux in toluene were required to achieve similar deprotonation

of the amido complexes **4** and **5**. The reaction was monitored by  $^1\text{H}$  NMR spectroscopy with a  $\text{C}_6\text{D}_6$  solution of **5** in a Teflon-valved NMR tube. Complete deprotonation was observed after 12 h of heating at  $120^\circ\text{C}$ , giving the bis(silylamido) compound **9** as the only reaction product. This reaction was reversible, however, and when the solution was cooled to room temperature, **9** reacted in solution with the eliminated amine  $\text{NHMe}_2$  to give the starting product **5** quantitatively, and so could not be isolated in this way. Nevertheless, pure **9** could be obtained at a preparative level when the same thermal treatment of **5** was carried out in a Teflon-valved Schlenk tube after addition of 1 equiv. of the monobenzylzirconium compound **11**, which reacts with amine in an irreversible reaction to give **9** with elimination of toluene (see Scheme 3). Similar deprotonation of the titanium compound **4** required heating at temperatures higher than  $160^\circ\text{C}$  to afford the bis(silylamido)titanium derivative **8**. This transformation was not quantitative, although pure **8** could be easily recovered because the reaction was not reversible on cooling to room temperature. Compounds **8** and **9** were isolated as brown and yellow solids, respectively, and identified by NMR spectroscopy.

Formation of the bis(silylamido) compounds is more selective, as it requires heating at temperatures above  $100^\circ\text{C}$ , except in the case of the benzylzirconium compound **11** ( $70^\circ\text{C}$ ). For the same reason the formation of the amidozirconium compound **9** is reversible in the presence of free amine.

The  $^1\text{H}$  and  $^{13}\text{C}$  NMR spectra of these diamido compounds **8–11** in  $\text{C}_6\text{D}_6$  are consistent with the presence of a plane of symmetry, making the two silylamido groups equivalent. They show one singlet ( $^1\text{H}$ ) and two resonances ( $^{13}\text{C}$ ) for the *t*Bu groups and two signals ( $^1\text{H}$  and  $^{13}\text{C}$ ) for the non-equivalent methyl groups of the  $\text{SiMe}_2$  moiety. Additionally, they show an  $\text{A}_2\text{B}$  spin system for the ring protons and three signals for the ring carbon atoms, along with one resonance for the methyl (**8**, **9**) and methylene (**10**, **11**) protons and carbon atoms of the  $\text{NMe}_2$  and  $\text{CH}_2\text{Ph}$  ligands, respectively. The  $\Delta\delta^{[15]}$  values are larger than those observed for non-coordinated  $\text{SiMe}_2\text{NHtBu}$  groups in monocyclopentadienyl (**2**, **3**) and single silylamido (**4–7**) compounds, but lower than those observed for the metal-coordinated  $\text{SiMe}_2\text{-}\eta^1\text{-NtBu}$  groups in silylamido compounds (**4–7**).

Orange crystals of **10** suitable for X-ray diffraction studies were isolated after extraction into hexane and slow cooling. The molecular structure of **10** is shown in Figure 1, and selected bond lengths and angles are listed in Table 1.

The titanium atom is in a pseudo-tetrahedral environment defined by the methylene carbon atom of the benzyl ligand, the centroid of the cyclopentadienyl ring, and the two coordinated nitrogen atoms of the silylamido groups. This is the first example of a neutral compound with a tridentate cyclopentadienyl ligand tethered by two silylamido groups.

Complex **10** shows  $\text{Ti}-\text{N}$  distances slightly longer than those reported for related  $[\text{Ti}\{\eta^5\text{-C}_5\text{R}_4\text{SiMe}_2(\eta^1\text{-NR}')\}\text{X}_2]$  compounds with only one silylamido ligand (1.907–1.919

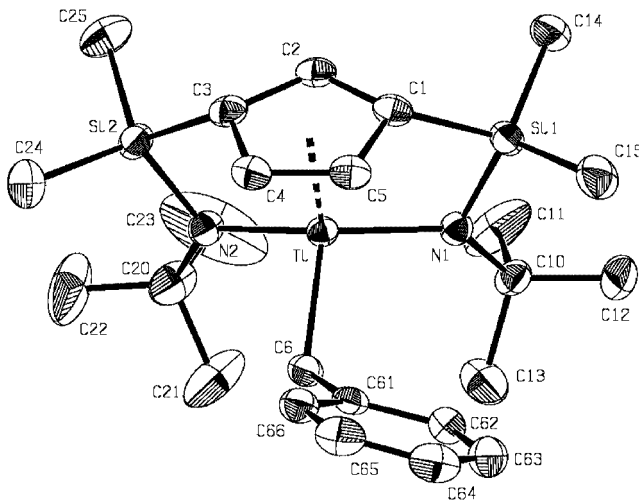


Figure 1. ORTEP drawing of the molecular structure of the major part of **10** in the solid state; thermal ellipsoids are drawn at the 50% probability level; the hydrogen atoms are omitted for clarity

Table 1. Selected interatomic distances [ $\text{\AA}$ ] and angles [ $^\circ$ ] for complexes [M = Ti (**10**), Zr (**13**)]; Cg denotes the centroid of the Cp ligand

	<b>10</b>	<b>13</b>
M–N1	1.9785(15)	2.0858(17)
M–N2	1.9808(15)	2.0812(17)
M–C1	2.3323(19)	2.4430(19)
M–C2	2.2915(18)	2.4062(2)
M–C3	2.3432(18)	2.4372(2)
M–C4	2.3885(18)	2.4672(2)
M–C5	2.381(2)	2.4662(2)
M–C6	2.1615(19)	
M…C32		3.019(2)
M–C33		2.571(3)
M…C34		3.057(3)
M–Cg	2.014	2.127
Si1–N1	1.7593(15)	1.7579(17)
Si1–C1	1.859(2)	1.865(2)
Si2–N2	1.7491(15)	1.7610(18)
Si2–C3	1.862(2)	1.870(2)
N1–M–N2	128.05(6)	126.89(7)
N1–M–C6	104.63(7)	
N1–M–C33		105.86(7)
N1–M–Cg	106.9	101.0
N2–M–C6	99.22(7)	
N2–M–C33		102.94(7)
N2–M–Cg	106.4	100.8
C6–M–Cg	111.0	
C33–M–Cg		121.1
Cg–C1–Si1	147.7	150.1
Cg–C3–Si2	146.9	150.5
C1–Si1–N1	93.70(8)	93.65(8)
C3–Si2–N2	93.92(8)	92.94(9)
M–N1–Si1	103.19(7)	105.56(8)
M–N2–Si2	103.53(8)	105.68(8)
M–C6–C61	124.25(13)	
M–C33–C32		94.56(15)
M–C33–C34		96.60(17)

$\text{\AA}$ )<sup>[2h,4g,16,17,18]</sup> but similar to the distance (1.971  $\text{\AA}$ )<sup>[19]</sup> reported for R = Me, R' = *t*Bu, X<sub>2</sub> = 2 NMe<sub>2</sub> (see Table 2). This behaviour would be consistent with a weaker  $\pi$ -bonding contribution from the interaction between the nitrogen p<sub>π</sub> orbital with the appropriate vacant metal d<sub>π</sub> orbital due to the presence of a second amido group, which simultaneously increases the steric crowding and strain of the bicyclic structure. In contrast, the Si–N and Si–C distances observed for **10** are very close to those observed for all single silylamido compounds. The Ti–Cg distance is in the lower range found for singly bridged silylamido compounds. There is no deviation of the disilyl-substituted cyclopentadienyl ligand from  $\eta^5$ -coordination, as deduced from the small differences in the Ti–C(ring) (2.347  $\text{\AA}$  average) and the C–C ring distances (1.419  $\text{\AA}$  average).

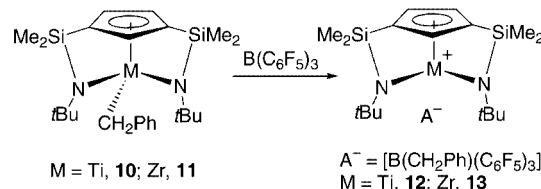
The amido nitrogen atom exhibits the expected planar disposition with sp<sup>2</sup> hybridization (the sum of bond angles around N is 360°) known for all structurally characterized silylamido complexes. The close Cg–C<sub>ring</sub>–Si angles (147.3° average) account for the strain in these bicyclic compounds. In addition, the Cg–Ti–N angles are similar, whereas the Ti–N–Si angles are significantly narrower and the C1–Si1–N angles more open than those found in single silylamido compounds. This is also consistent with the differences observed in the bond lengths for a system in which the Si–N distances do not change whereas the Ti–N distances are longer. The N1–Ti–N2 angle is very open. The Ti–C<sub>6</sub> distance is in the known range for benzyltitanium compounds.

The most significant structural feature of **10** is the orientation of the benzyl ligand, with its phenyl ring directed toward the cyclopentadienyl ring (see DFT calculations be-

low). A similar orientation has also recently been observed for [Ti{1,3-[CH<sub>2</sub>(2-C<sub>4</sub>H<sub>3</sub>N)]}]<sub>2</sub>( $\eta^5$ -C<sub>5</sub>H<sub>3</sub>)(NMe<sub>2</sub>)].<sup>[20]</sup>

### Cationic Compounds

Addition of C<sub>6</sub>D<sub>6</sub> by vacuum transfer to a Teflon-valved NMR tube containing a mixture of B(C<sub>6</sub>F<sub>5</sub>)<sub>3</sub> and the benzyl compounds **10** or **11** in a 1:1 molar ratio immediately gave the partially soluble cationic species [M( $\eta^5$ -C<sub>5</sub>H<sub>3</sub>(SiMe<sub>2</sub>– $\eta^1$ -N*t*Bu))]<sup>+</sup>, isolated as [B(CH<sub>2</sub>Ph)(C<sub>6</sub>F<sub>5</sub>)<sub>3</sub>]<sup>–</sup> salts **12** and **13** as orange solids, which were identified by NMR spectroscopy and X-ray diffraction studies.



Scheme 4. Formation of cationic bis(amidosilyl)cyclopentadienyl complexes

The structures of the cations in C<sub>6</sub>D<sub>6</sub> solutions were established by NMR studies. Their <sup>1</sup>H and <sup>13</sup>C NMR spectra are consistent with the C<sub>s</sub> symmetry also observed for the neutral benzyl precursor compounds **10** and **11**. They each show one singlet (<sup>1</sup>H) and two resonances (<sup>13</sup>C) for the *t*Bu groups, two signals (<sup>1</sup>H and <sup>13</sup>C) for non-equivalent methyl groups of the SiMe<sub>2</sub> groups, an A<sub>2</sub>B spin system for the ring protons and three signals for the ring carbon atoms.

Table 2. Selected bond lengths [ $\text{\AA}$ ] and bond angles [ $^\circ$ ] for related complexes

Compound	M–N	M–Cg <sup>[a]</sup>	Cg–M–N	M–C	Si–N	Ref.
Ti[(C <sub>5</sub> Me <sub>4</sub> )SiMe <sub>2</sub> ( $\eta^1$ -NBz)]Bz <sub>2</sub>	1.919	2.045	107.4	2.131 2.158	1.731	[16]
Ti[(C <sub>5</sub> Me <sub>4</sub> )(SiMe <sub>2</sub> { $\eta^1$ -NCHMePh})] Cl(CH <sub>2</sub> SiMe <sub>3</sub> )	1.909(3)	2.030	107.2	2.106(5)		[17]
Ti[(C <sub>5</sub> H <sub>4</sub> )SiMe <sub>2</sub> ( $\eta^1$ -NAr)]Cl <sub>2</sub>	1.914(3)	2.016	105.1		1.755(3)	[2h]
Ti[(C <sub>5</sub> H <sub>4</sub> )SiMe <sub>2</sub> ( $\eta^1$ -NAr){CH <sub>2</sub> B(C <sub>6</sub> F <sub>5</sub> ) <sub>2</sub> } (C <sub>6</sub> F <sub>5</sub> )]	1.911(4)	2.033	105.3	2.169(5)	1.749(4)	[4g]
Ti[(C <sub>5</sub> Me <sub>4</sub> )SiMe <sub>2</sub> ( $\eta^1$ -N <i>t</i> Bu)]Cl <sub>2</sub>	1.907(4)	2.030	107.6			[19]
Ti[(C <sub>5</sub> Me <sub>4</sub> )SiMe <sub>2</sub> ( $\eta^1$ -N <i>t</i> Bu)][(NMe <sub>2</sub> ) <sub>2</sub>	1.972(4) 1.924(5) 1.906(4)	2.083	105.5		1.722(4)	[19]
Ti(C <sub>5</sub> Me <sub>5</sub> )(NMe <sub>2</sub> ) <sub>3</sub>	1.919(9)	2.132	119.4			[18]
Ti[C <sub>5</sub> H <sub>3</sub> {SiMe <sub>2</sub> ( $\eta^1$ -N <i>t</i> Bu)} <sub>2</sub> ](CH <sub>2</sub> Ph)	1.9785(15) 1.9808(15)	2.014 2.016	106.9 106.4	2.1615(19)	1.7593(15) 1.7491(15)	
[Ti{C <sub>5</sub> H <sub>3</sub> [SiMe <sub>2</sub> ( $\eta^1$ -N <i>t</i> Bu)]} <sub>2</sub> ] <sup>+</sup> [(CH <sub>2</sub> Ph)B(C <sub>6</sub> F <sub>5</sub> ) <sub>3</sub> ] <sup>–</sup>	1.959(4) 1.946(5)	1.997(5) 2.000(5)	106.7 106.6	2.447(3)	1.773(5) 1.788(5)	[7]
Zr[(C <sub>5</sub> Me <sub>4</sub> )SiMe <sub>2</sub> ( $\eta^1$ -N <i>t</i> Bu)][(NMe <sub>2</sub> ) <sub>2</sub>	2.108(4) <sup>[b]</sup> 2.060(5) 2.064(4)	2.233	100.2		1.730(4)	[19]
Zr[(C <sub>5</sub> H <sub>3</sub> ) {SiMe <sub>2</sub> ( $\eta^1$ -N <i>t</i> Bu)} {SiMe <sub>2</sub> (NMe <sub>2</sub> )}]Cl(CH <sub>3</sub> )	2.078	2.198	101.0	2.311 2.232(3) 2.248(3)	1.742 1.738	[21]
Zr[(C <sub>13</sub> H <sub>8</sub> )SiMe <sub>2</sub> ( $\eta^1$ -N <i>t</i> Bu)][(CH <sub>2</sub> SiMe <sub>3</sub> ) <sub>2</sub>	2.061(2)					[22]
[Zr{C <sub>5</sub> H <sub>3</sub> [SiMe <sub>2</sub> ( $\eta^1$ -N <i>t</i> Bu)]} <sub>2</sub> ] <sup>+</sup> [(CH <sub>2</sub> Ph)B(C <sub>6</sub> F <sub>5</sub> ) <sub>3</sub> ] <sup>–</sup>	2.0858(17) 2.0812(17)	2.127 2.127	101.0 100.8	2.571(3)	1.7579(17) 1.7610(18)	

<sup>[a]</sup> Cg denotes the centroid of the cyclopentadienyl ring. <sup>[b]</sup> The M–N bond of the silylamido bridge.

The  $\Delta\delta^{[15]}$  values for the *t*Bu  $^{13}\text{C}$  signals are slightly larger than those observed for corresponding neutral compounds. A surprising effect is observed when the  $^1\text{H}$  and  $^{13}\text{C}$  NMR spectra of the neutral benzyl precursor compounds **10–11** are compared with those of the corresponding cationic titanium and zirconium derivatives **12–13**: all of the NMR resonances for the cationic species are shifted upfield. It is also remarkable that this effect is particularly important for the ring CH proton located between the two silyl substituents. Furthermore, it is interesting to note that the ring  $C_{ipso}$  resonance is the signal at highest field for the neutral compounds whereas for the cationic derivatives it appears between the other two ring C resonances. This unexpected behaviour seems to be associated with the anisotropy of the benzyl ring exerted in the particular structure of these cationic species.

Orange crystals of **13**, appropriate for a single-crystal X-ray structure determination, were isolated from a  $\text{C}_6\text{D}_6$  solution in the NMR tube. A perspective view of the molecular structure of **13** is shown in Figure 2, along with the non-hydrogen labelling scheme, and selected bond lengths and angles are listed in Table 1.

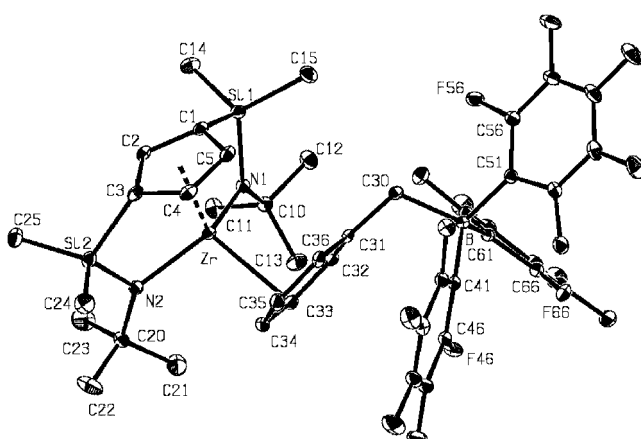


Figure 2. ORTEP drawing of the molecular structure of **13** in the solid state; thermal ellipsoids are drawn at the 10% probability level and hydrogen atoms are omitted for clarity

The pseudo-tetrahedral geometry about the Zr atom of **13** is defined by the centroid of the cyclopentadienyl ring and the two N-donors of the appended (dimethylsilyl)amido arms, with the remaining coordination site occupied by C(33) of the phenyl ring of the benzylborate anion. This disposition is very close to that observed for complex **12**<sup>[7]</sup> with the expected longer Zr–N and similar Si–N [1.773(5) Å; 1.788(5) Å for **12**] bonds. In comparison with those in the related neutral  $[\text{Zr}\{(\eta^5-\text{C}_5\text{R}_4)\text{SiMe}_2(\eta^1-\text{NR}')\}\text{X}_2]$  compounds containing only one silylamido ligand, the Zr–N distances in **13** are similar,<sup>[21,22]</sup> but slightly shorter than the distances reported<sup>[19]</sup> for R = Me, R' = *t*Bu, X<sub>2</sub> = 2 NMe<sub>2</sub>. This behaviour is consistent with a similar  $\pi$ -bonding contribution from the two amido ligands to the more acidic zirconium cation. The Cg–Zr distance is significantly shorter than those observed in related single silylamido neu-

tral complexes (see Table 2), indicating higher electron donation from the cyclopentadienyl ring.

The amido nitrogen atom exhibits the expected planar disposition with  $\text{sp}^2$  hybridization (the sum of bond angles around N is 360°) known for all reported silylamido complexes. The constrained geometry of the Cg–C<sub>ring</sub>–Si–N–Zr cyclic systems is similar to that found for **12**. The ring C1 and C3 atoms, bearing the amidosilyl arms, are pyramidal distorted almost to the same extent, as shown by the sums of their bond angles (349.4° average) and by the Cg–C<sub>ring</sub>–Si angles (150.3° average). The angles at Si and N are in the range found for **12**, whereas the Cg–Zr–N angles (100.9° average) are significantly narrower than those observed in the related titanium cation **12** (106.65° average). This is consistent with the increased atomic radius of the Zr centre and is responsible for the slightly more constrained geometry shown by **13**.

The Zr–C33 bond [2.571(3) Å] is about 0.30 Å longer, whereas the distances to the neighbouring C32 and C34 atoms are about 0.8 Å longer than those observed for covalent Zr–C bonds, indicating an interaction of the empty hybrid metal orbital with the  $p_\pi$  orbital of the *meta*-C<sub>phenyl</sub> atom of the borate anion.<sup>[23]</sup> The most significant feature of this structure is that the phenyl ring is oriented upward in the direction of the cyclopentadienyl ring, as also observed for the benzyl substituent in complex **10**.

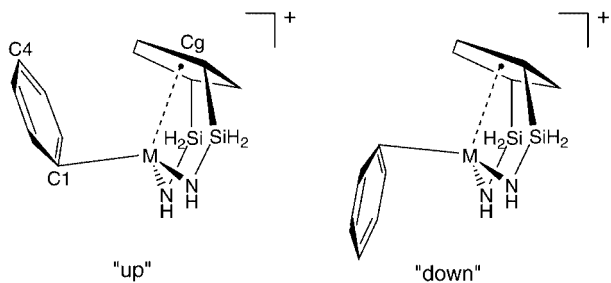
### Structure and Bonding of $[\text{Ti}\{\eta^5-\text{C}_5\text{H}_3(\text{SiMe}_2-\eta^1-\text{NtBu})_2\}]^+$ Cations

In this section we present density functional calculations performed on the model compound  $[\text{Ti}\{\eta^5-\text{C}_5\text{H}_3(\text{SiH}_2-\eta^1-\text{NH})_2\}]^+$  as well as on the real molecule  $[\text{Ti}\{\eta^5-\text{C}_5\text{H}_3(\text{SiMe}_2-\eta^1-\text{NtBu})_2\}]^+$ . The calculations for the model system serve to establish characteristic patterns in chemical bonding for bis(amidosilyl)cyclopentadienyl compounds of Ti and Zr. As mentioned above, these compounds can reasonably be regarded as 14-electron species, due to inclusion of the amido  $\pi$ -electrons. In the light of our previous analysis,<sup>[8c]</sup> we can expect that the bonding of  $[\text{Ti}\{\eta^5-\text{C}_5\text{H}_3(\text{SiR}_2-\eta^1-\text{NR})_2\}]^+$  cations should be governed by electrostatic interaction and ligand-to-metal donation, whereas back-bonding should play an only minor role.

### Bonding of the Model System $[\text{Ti}\{\eta^5-\text{C}_5\text{H}_3(\text{SiH}_2-\eta^1-\text{NH})_2\}]^+$

We first performed DFT calculations on the species with aryl ligands,  $[\text{Ti}\{\eta^5-\text{C}_5\text{H}_3(\text{SiH}_2-\eta^1-\text{NH})_2\}]^+[\eta^x-\text{C}_6\text{H}_5\text{R}]$  (R = H, CH<sub>3</sub>, CH<sub>2</sub>BF<sub>3</sub><sup>-</sup>; x = 1, 2). For benzene, we considered different “up” and “down” coordination modes, as indicated in Scheme 5. For  $\eta^1$ -coordination, “up” and “down” coordination modes are characterized by dihedral angles (C4–C1–M–Cg) close to 0 and 180°, respectively, C1 being the benzene carbon atom coordinating to the metal centre, and C4 being the benzene carbon atom in the position *para* to C1. Similarly, for  $\eta^2$ -coordination, dihedral angles (X4–X1–M–Cg) close to 0 and 180° characterize “up” and “down” coordination modes, X1 being the mid-

point between the two coordinating benzene carbon atoms, and X4 being the midpoint of the two corresponding benzene carbon atoms in the *para* position.



Scheme 5. The “up” and “down” coordination modes of the solvated model cation  $[\text{Ti}\{\text{C}_5\text{H}_3(\text{SiH}_2\text{NH})_2\}]^+$

The optimized geometry of the naked cation  $[\text{Ti}\{\eta^5\text{C}_5\text{H}_3(\text{SiH}_2\text{-}\eta^1\text{-NH})_2\}]^+$  and its main empty frontier molecular orbital are displayed in Figure 3. The HOMO of the aryl ligand, dominates the orbital interaction through donation to the empty  $d_{z^2}$  orbital at the metal centre.

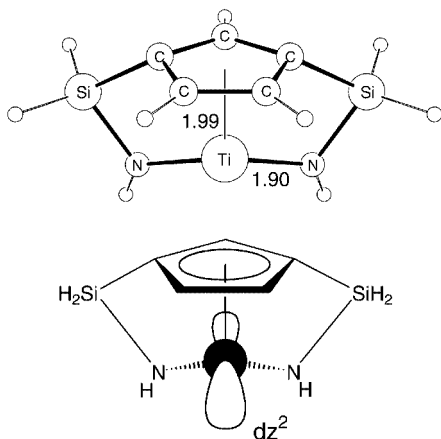


Figure 3. Optimized geometry for the model cation  $[\text{Ti}\{\text{C}_5\text{H}_3(\text{SiH}_2\text{NH})_2\}]^+$  and a main empty frontier MO

We recall from simple Hückel considerations that the HOMO of benzene consists of a set of degenerate  $e_{1g}$  orbitals, one of which is more likely to undergo  $\eta^1$ -type donation, whereas the other would induce a preference for  $\eta^2$ -coordination. For toluene, the degeneracy of the  $e_{1g}$  set is lifted, due to the antibonding hyperconjugation of the methyl group. In this case, the HOMO is most suited to  $\eta^1$ -coordination, having the largest orbital coefficient at the

ring carbon atom in the position *para* to the methyl substituent.

The relative energies for various investigated complex geometries, together with optimized Ti–L bond lengths, are collected in Table 3. Relative energies are determined for groups of isomeric compounds, in which the energy of the isomer with the largest absolute value in total bonding energy is set to zero, and energies of isomers are reported with reference to the energy of the isomer at zero energy.

The energy differences are small, but significant. In particular, we note that  $\eta^1$ -coordination is favoured for the cationic complexes by about 10 kJ/mol. The small energy differences are accompanied by a fairly large change in the Ti–C bond length, of about 0.20 Å, indicating the subtle nature of this bonding interaction. The bond energies (BEs) of benzene and toluene amount to 89 kJ/mol and 100 kJ/mol, respectively.

Finally, complexes of the borate anion  $\text{C}_6\text{H}_5\text{CH}_2\text{BF}_3^-$  are characterized by the Ti–C bonds, which are about 0.20 Å shorter than those in the related benzene or toluene complexes. Electrostatic interactions between the anionic ligand and the cationic metal fragment have a pronounced influence on the Ti–L bond strength. Again,  $\eta^1$ -coordination is favoured by 16 kJ/mol.

### Complexes with the Cation $[\text{Ti}\{\eta^5\text{C}_5\text{H}_3(\text{SiMe}_2\text{-}\eta^1\text{-NtBu})_2\}]^+$

We begin with the molecular geometry of  $[\text{Ti}\{\eta^5\text{C}_5\text{H}_3(\text{SiMe}_2\text{-}\eta^1\text{-NtBu})_2\}\{\eta^1\text{-C}_6\text{H}_5\text{CH}_2\text{B}(\text{C}_6\text{F}_5)_3\}]$ , which has also been established by crystal structure determination.<sup>[7]</sup> By our analysis, we can expect the following features for this compound. Firstly, the  $[\text{C}_6\text{H}_5\text{CH}_2\text{B}(\text{C}_6\text{F}_5)_3]^-$  borate ligand should coordinate in  $\eta^1$ -fashion, being oriented upwards toward the site of the cyclopentadienyl ring. This structural feature is observed in the crystal structure of this compound. Furthermore, from simple Hückel orbital considerations, we expect that the coordinating ring carbon atom should be located *para* to the boron substituent. However, the solid-state structure reveals coordination through a *meta* carbon atom rather than one in the *para* position. We therefore optimized two representative geometries for both *meta* and *para* coordination, as shown in Figure 4.

For the *meta* coordination (Figure 4, a), inspection of the optimized geometries reveals the presence of short F···H distances ( $d \approx 2.40$  Å), between the pentafluorophenyl rings and methyl groups of the metal fragment. For *para* coordi-

Table 3. Relative energies [kJ/mol] and metal-to-ligand bond lengths [Å] for coordination of the aryl double bond for various complexes of the type  $[\{\text{C}_5\text{H}_3(\text{SiH}_2\text{NH})_2\}\text{Ti}]^+[\eta^x\text{-C}_6\text{H}_5\text{R}]$  ( $\text{R} = \text{H}, \text{CH}_3, \text{CH}_2\text{BF}_3^-; x = 1, 2$ )

	R = H				R = Me		R = $\text{CH}_2\text{BF}_3^-$	
	$\eta^1$ “up” <sup>[c]</sup>	$\eta^1$ “down”	$\eta^2$ “up”	$\eta^2$ “down”	$\eta^1$ “up”	$\eta^2$ “up”	$\eta^1$ “up”	$\eta^2$ “up”
$E_{\text{rel}}^{[a]}$	0	6	9	8	0	12	0	16
$d(\text{Ti}-\text{C})^{[b]}$	2.46	2.54	2.69	2.66	2.43	2.67, 2.69	2.28	2.41, 2.66

[a] The most stable isomer is set to zero. [b] Bond lengths between the  $\text{C}_6\text{H}_5\text{R}$  ligand and the metal centre. [c] See Scheme 5 for a definition of “up” and “down” coordination.

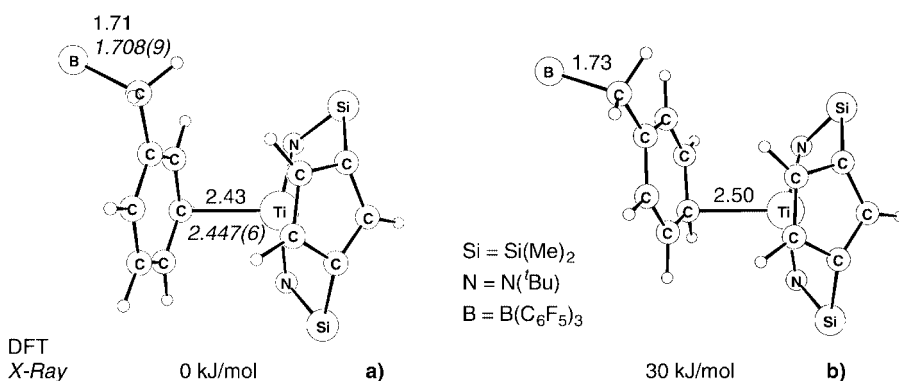


Figure 4. Relative energies and selected bond lengths for *meta* (a) and *para* coordination (b) of  $[\text{Ti}\{\eta^5\text{-C}_5\text{H}_3(\text{SiMe}_2\text{N}^t\text{Bu})_2\}\{\eta^1\text{-C}_6\text{H}_5\text{CH}_2\text{B}(\text{C}_6\text{F}_5)_3\}]$ ; comparison with X-ray analysis

nation (Figure 4, b), in contrast, no such short contacts can be found. The presence of such intramolecular hydrogen bonds might be the key point that explains why the *meta* geometry is energetically favoured by 30 kJ/mol. To produce further evidence for our argument, we also optimized *meta* and *para* geometries for  $[\text{Ti}\{\eta^5\text{-C}_5\text{H}_3(\text{SiMe}_2\text{-}\eta^1\text{-N}^t\text{Bu})_2\}\{\eta^1\text{-C}_6\text{H}_5\text{CH}_2\text{BF}_3\}]$ . As was to be expected, since no short F...H contacts can be achieved in this case, orbital interactions now favour the latter coordination mode by 13 kJ/mol.

We then optimized the molecular geometry of  $[\text{Ti}\{\eta^5\text{-C}_5\text{H}_3(\text{SiMe}_2\text{-}\eta^1\text{-N}^t\text{Bu})_2\}(\text{CH}_2\text{C}_6\text{H}_5)]$ , which is displayed in Figure 5. The geometry of the neutral benzyl complex again exhibits “up” coordination, with a typical Ti–C bond length of 2.19 Å. The optimized geometry is in good agreement with the crystal structure of this compound. The reaction energy ( $\Delta E$ ) for the formation of the benzyl complex from  $[\text{Ti}\{\eta^5\text{-C}_5\text{H}_3(\text{SiMe}_2\text{-}\eta^1\text{-N}^t\text{Bu})_2\}\{\eta^1\text{-C}_6\text{H}_5\text{CH}_2\text{B}(\text{C}_6\text{F}_5)_3\}]$ , which involves the cleavage of a C–B bond, followed by a reorientation of the benzyl fragment, amounts to  $-15$  kJ/mol. The latter compound is therefore stable for kinetic, but not for thermodynamic, reasons. One factor

lending kinetic stability to the unusual  $\eta^1$ -adduct is the energy of preparation of the  $\text{B}(\text{C}_6\text{F}_5)_3$  fragment, associated with the pyramidalization of the trigonal-planar-coordinated boron atom, which substantially increases the value for the C–B bond strength by the order of 80 kJ/mol.<sup>[8c]</sup>

## Conclusion

To conclude, we have synthesized a new type of  $[\text{bis}(\eta^1\text{-amidosilyl})\text{cyclopentadienyl}]\text{titanium}$  and -zirconium complexes by direct deprotonation of the corresponding bis(aminosilyl)cyclopentadiene with metal tetraamide and tetra-benzyl derivatives under varying thermal conditions. The complexes obtained in this way may be classified into three categories: monocyclopentadienyl, *ansa*-(amidosilyl)cyclopentadienyl and *bis[ansa*-(amidosilyl)cyclopentadienyl] complexes. The first two categories show the structures and chemical behaviour expected for these well-known types of compounds. However, the *bis[ansa*-bis(amidosilyl)cyclopentadienyl] complexes are isolobal with previously reported tris(cyclopentadienyl) compounds and present reactivity pathways determined by the strong electrostatic character of the interactions, additionally facilitated by the unique accessible metal orbital. Treatment of the benzyl complexes with  $\text{B}(\text{C}_6\text{F}_5)_3$  gave the cationic species, which were characterized by X-ray diffraction methods, indicating that the counter-ion is coordinated to the metal atom through a single interaction with the phenyl *m*-carbon atom of the benzyl borate anion.

Density functional calculations developed for the cationic complexes provide an explanation for their remarkable structural features, particularly the “up” (oriented toward the cyclopentadienyl ring) coordination of the benzyl group in the neutral benzyltitanium complex and of the ligand (solvent or counter-anion) bound in the cationic species.

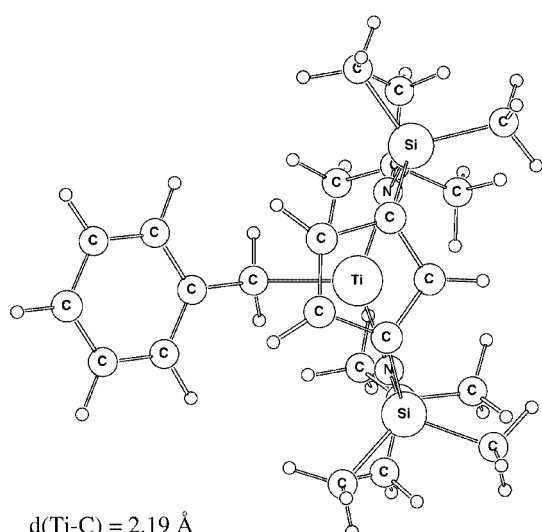


Figure 5. Optimized geometry of the benzyl complex  $[\text{Ti}\{\eta^5\text{-C}_5\text{H}_3(\text{SiMe}_2\text{N}^t\text{Bu})_2\}(\text{CH}_2\text{C}_6\text{H}_5)]$

## Experimental Section

**General Remarks:** All experiments were carried out under argon by use either of a Vacuum Atmospheres glove box or of standard Schlenk techniques. Hydrocarbon solvents and THF were distilled from Na/benzophenone and stored under argon prior to use.

1,1-Bis(chlorodimethylsilyl)cyclopentadiene,  $Ti(NMe_2)_4$ ,<sup>[11]</sup>  $Zr(NMe_2)_4$ ,<sup>[11]</sup>  $Ti(CH_2Ph)_4$ ,<sup>[12]</sup>  $Zr(CH_2Ph)_4$ ,<sup>[12]</sup> and  $B(C_6F_5)_3$ ,<sup>[24]</sup> were prepared by previously reported methods. NMR spectra were recorded with Varian Unity FT 300 and Varian FT 500 Unity Plus instruments in Teflon-valved tubes at probe temperature (20 °C).  $^1H$  and  $^{13}C$  NMR chemical shifts were measured relative to the residual resonances of  $C_6D_6$  used as solvent, but the chemical shifts are reported with respect to TMS.  $^{19}F$  NMR chemical shifts are referenced to external  $CFCl_3$ . Coupling constants are reported in Hz. C, H and N analyses were carried out with a Perkin–Elmer 240 C analyzer.

**C<sub>5</sub>H<sub>4</sub>(SiMe<sub>2</sub>NH<sub>t</sub>Bu)<sub>2</sub>** (**1**): A solution of  $LiNH_{t}Bu$  (1.61 g, 20.5 mmol) in THF (40 mL) was added at 0 °C to a solution of  $C_5H_4\cdot 1,1-(SiMe_2Cl)_2$  (2.51 g, 10 mmol) in THF and the mixture was stirred for 12 h. The volatiles were removed under vacuum and the residue was extracted into hexane to give a mixture of isomers of **1** as a yellow liquid after removal of the solvent (2.92 g, 9.0 mmol, 90%).  $^1H$  NMR ( $C_6D_6$ , 20 °C) of the major component (**1a**):  $\delta = -0.05$  (br. s, 6 H, SiMe<sub>2</sub>), 0.21 (br. s, 6 H, SiMe<sub>2</sub>), 1.12 (s, 9 H, NH<sub>t</sub>Bu), 1.17 (s, 9 H, NH<sub>t</sub>Bu), 3, 57 (m, 1 H, CpH), 6.50 (m, 1 H,  $C_5H_3$ ), 6.71 (m, 2 H,  $C_5H_3$ ) ppm. Component **1b**:  $\delta = 0.09$  (s, 12 H, SiMe<sub>2</sub>), 1.15 (s, 18 H, NH<sub>t</sub>Bu), 6.53 (m, 2 H,  $C_5H_4$ ), 6.78 (m, 2 H,  $C_5H_4$ ) ppm.

**[Ti{ $\eta^5$ -C<sub>5</sub>H<sub>3</sub>-1,3-[SiMe<sub>2</sub>(NH<sub>t</sub>Bu)]<sub>2</sub>}(NMe<sub>2</sub>)<sub>3</sub>**] (**2**): A solution of  $Ti(NMe_2)_4$  (0.65 g, 2.9 mmol) in toluene (70 mL) was cooled to 0 °C, and **1** (0.94 g, 2.9 mmol) was added by syringe. The resulting red solution was stirred at 50 °C for 5 h. When the evolution of gas had stopped, the solvent was removed under vacuum and the residue was extracted into pentane (70 mL). After filtration and removal of the solvent, complex **2** was isolated as a deep red oil (1.45 g, 2.8 mmol, 97%).  $^1H$  NMR ( $C_6D_6$ , 20 °C):  $\delta = 0.41$  (s, 6 H, SiMe<sub>2</sub>), 0.43 (s, 6 H, SiMe<sub>2</sub>), 1.04 (s, 2 H, NH<sub>t</sub>Bu), 1.16 (s, 18 H, NH<sub>t</sub>Bu), 3.13 (s, 18 H, NMe<sub>2</sub>), 6.31 (d, 2 H,  $C_5H_3$ ), 6.60 (t, 1 H,  $C_5H_3$ ) ppm.  $^{13}C$  NMR ( $C_6D_6$ , 20 °C):  $\delta = 2.9$  (SiMe<sub>2</sub>), 4.1 (SiMe<sub>2</sub>), 34.0 (NtBu), 49.3 (NtBu<sub>tert</sub>), 50.3 (NMe<sub>2</sub>), 119.9 ( $C_5H_3$ ), 125.2 ( $C_5H_3$ ), 127.8 ( $C_5H_3$ ) ppm. IR (Nujol):  $\tilde{\nu} = 3383$  (N–H) cm<sup>-1</sup>.  $C_{23}H_{53}N_5Si_2Ti$  (503.76): calcd. C 54.84, H 10.60, N 13.09; found C 54.17, H 10.23, N 12.82.

**[Zr{ $\eta^5$ -C<sub>5</sub>H<sub>3</sub>-1,3-[SiMe<sub>2</sub>(NH<sub>t</sub>Bu)]<sub>2</sub>}(NMe<sub>2</sub>)<sub>3</sub>**] (**3**): Compound **1** (0.05 g, 0.1 mmol) was added by syringe to a solution of  $Zr(NMe_2)_4$  (0.041 g, 0.1 mmol) in  $C_6D_6$  (0.6 mL). Complex **3** was immediately identified in the NMR spectrum as the unique product of the reaction.  $^1H$  NMR ( $C_6D_6$ , 20 °C):  $\delta = 0.42$  (s, 6 H, SiMe<sub>2</sub>), 0.44 (s, 6 H, SiMe<sub>2</sub>), 1.08 (s, 2 H, NH<sub>t</sub>Bu), 1.15 (s, 18 H, NtBu), 2.98 (s, 18 H, NMe<sub>2</sub>), 6.50 (d, 2 H,  $C_5H_3$ ), 6.78 (t, 1 H,  $C_5H_3$ ) ppm.  $^{13}C$  NMR ( $C_6D_6$ , 20 °C):  $\delta = 2.8$  (SiMe<sub>2</sub>), 3.5 (SiMe<sub>2</sub>), 33.9 (NtBu), 45.6 (NMe<sub>2</sub>), 49.3 (NtBu<sub>tert</sub>), 120.5 ( $C_5H_3$ ), 127.0 ( $C_5H_3$ ), 127.2 ( $C_5H_3$ ) ppm. Pure **3** was only observed in NMR-tube experiments, while solid samples were always contaminated by small amounts of **5**.

**[Ti{ $\eta^5$ -C<sub>5</sub>H<sub>3</sub>-1-[SiMe<sub>2</sub>(NH<sub>t</sub>Bu)]-3-[SiMe<sub>2</sub>( $\eta^1$ -NtBu)}(NMe<sub>2</sub>)<sub>2</sub>**] (**4**): A solution of  $Ti(NMe_2)_4$  (2.00 g, 8.9 mmol) in toluene (70 mL) was cooled to 0 °C, and **1** (2.91 g, 8.9 mmol) was added by syringe. The resulting red solution was heated at reflux for 5 h. When the evolution of gas had stopped, the solvent was removed under vacuum and the residue was extracted into pentane (70 mL). After filtration and removal of the solvent, complex **4** was isolated as a deep red oil (4.10 g, 8.8 mmol, 98%).  $^1H$  NMR ( $C_6D_6$ , 20 °C):  $\delta = 0.35$  (s, 3 H, SiMe<sub>2</sub>NtBu), 0.43 (s, 3 H, SiMe<sub>2</sub>NH<sub>t</sub>Bu), 0.50 (s, 3 H, SiMe<sub>2</sub>NtBu), 0.54 (s, 3 H, SiMe<sub>2</sub>NtBu), 0.86 (s, 1 H, NH<sub>t</sub>Bu), 1.12 (s, 9 H, NH<sub>t</sub>Bu), 1.28 (s, 9 H, NtBu), 2.87 (s, 6 H, NMe<sub>2</sub>), 3.05 (s,

6 H, NMe<sub>2</sub>), 6.12 (m, 1 H,  $C_5H_3$ ), 6.31 (m, 1 H,  $C_5H_3$ ), 6.50 (m, 1 H,  $C_5H_3$ ) ppm.  $^{13}C$  NMR ( $C_6D_6$ , 20 °C):  $\delta = 2.1$  (SiMe<sub>2</sub>), 2.4 (SiMe<sub>2</sub>), 2.4 (SiMe<sub>2</sub>), 3.7 (SiMe<sub>2</sub>), 34.1 (NH<sub>t</sub>Bu), 34.4 (NtBu), 49.1 (NMe<sub>2</sub>), 49.6 (NH<sub>t</sub>Bu<sub>tert</sub>), 50.4 (NMe<sub>2</sub>), 60.8 (NtBu<sub>tert</sub>), 109.1 ( $C_5H_3$ ), 121.2 ( $C_5H_3$ ), 122.5 ( $C_5H_3$ ), 123.7 ( $C_5H_3$ ), 130.7 ( $C_5H_3$ ) ppm. IR (Nujol):  $\tilde{\nu} = 3385$  (N–H) cm<sup>-1</sup>.  $C_{21}H_{46}N_4Si_2Ti$  (458.67): calcd. C 54.99, H 10.11, N 12.21; found C 54.67, H 9.97, N 12.04.

**[Zr{ $\eta^5$ -C<sub>5</sub>H<sub>3</sub>-1-[SiMe<sub>2</sub>(NH<sub>t</sub>Bu)]-3-[SiMe<sub>2</sub>( $\eta^1$ -NtBu)}](NMe<sub>2</sub>)<sub>2</sub>** (**5**): A solution of  $Zr(NMe_2)_4$  (3.37 g, 12.6 mmol) in toluene (70 mL) was cooled to 0 °C, and **1** (4.09 g, 12.6 mmol) was added by syringe. The resulting yellow solution was warmed to 65 °C for 5 h. When the evolution of gas had stopped, the solvent was removed under vacuum and the residue was extracted into pentane (70 mL). After filtration and removal of the solvent, complex **5** was isolated as a light brown solid (6.19 g, 12.3 mmol, 98%). IR (Nujol):  $\tilde{\nu} = 3384$  (N–H) cm<sup>-1</sup>.  $^1H$  NMR ( $C_6D_6$ , 20 °C):  $\delta = 0.35$  (s, 3 H, SiMe<sub>2</sub>NH<sub>t</sub>Bu), 0.42 (s, 3 H, SiMe<sub>2</sub>NH<sub>t</sub>Bu), 0.57 (s, 3 H, SiMe<sub>2</sub>NtBu), 0.59 (s, 3 H, SiMe<sub>2</sub>NtBu), 0.85 (s, 1 H, NH<sub>t</sub>Bu), 1.11 (s, 9 H, NH<sub>t</sub>Bu), 1.27 (s, 9 H, NtBu), 2.81 (s, 6 H, NMe<sub>2</sub>), 2.82 (s, 6 H, NMe<sub>2</sub>), 6.39 (m, 1 H,  $C_5H_3$ ), 6.47 (m, 1 H,  $C_5H_3$ ), 6.69 (m, 1 H,  $C_5H_3$ ) ppm.  $^{13}C$  NMR ( $C_6D_6$ , 20 °C):  $\delta = 2.3$  (SiMe<sub>2</sub>), 2.7 (SiMe<sub>2</sub>), 2.8 (SiMe<sub>2</sub>), 3.0 (SiMe<sub>2</sub>), 33.9 (NH<sub>t</sub>Bu), 34.9 (NtBu), 44.2 (NMe<sub>2</sub>), 44.5 (NMe<sub>2</sub>), 49.6 (NH<sub>t</sub>Bu<sub>tert</sub>), 56.6 (NtBu<sub>tert</sub>), 111.4 ( $C_5H_3$ ), 122.6 ( $C_5H_3$ ), 122.9 ( $C_5H_3$ ); 124.7 ( $C_5H_3$ ), 126.7 ( $C_5H_3$ ) ppm.  $C_{21}H_{46}N_4Si_2Zr$  (502.01): calcd. C 50.24, H 9.24, N 11.16; found C 49.73, H 9.05, N 11.45.

**[Ti{ $\eta^5$ -C<sub>5</sub>H<sub>3</sub>-1-[SiMe<sub>2</sub>(NH<sub>t</sub>Bu)]-3-[SiMe<sub>2</sub>( $\eta^1$ -NtBu)}](CH<sub>2</sub>Ph)<sub>2</sub>** (**6**): A solution of  $Ti(CH_2Ph)_4$  (2.14 g, 5.2 mmol) in toluene (70 mL) was cooled to 0 °C, and **1** (1.69 gr, 5.2 mmol) was added by syringe. The resulting yellow solution was warmed to 70 °C for 5 h. When the evolution of gas had stopped, the solvent was removed under vacuum and the residue was extracted into pentane (70 mL). After filtration and removal of the solvent, complex **6** was isolated as a red-brown solid (2.86 g, 5.1 mmol, 98%).  $^1H$  NMR ( $C_6D_6$ , 20 °C):  $\delta = 0.21$  (s, 3 H, SiMe<sub>2</sub>NH<sub>t</sub>Bu), 0.27 (s, 3 H, SiMe<sub>2</sub>NH<sub>t</sub>Bu), 0.37 (s, 3 H, SiMe<sub>2</sub>NtBu), 0.38 (s, 3 H, SiMe<sub>2</sub>NtBu), 0.72 (s, 1 H, NH<sub>t</sub>Bu), 1.06 (s, 9 H, NH<sub>t</sub>Bu), 1.44 (s, 9 H, NtBu), 2.46 (d,  $J = 10.5$  Hz, 1 H,  $CH_2Ph$ ), 2.55 (d,  $J = 10.5$  Hz, 1 H,  $CH_2Ph$ ), 2.81 (d,  $J = 10.5$  Hz, 1 H,  $CH_2Ph$ ), 2.97 (d,  $J = 10.5$  Hz, 1 H,  $CH_2Ph$ ), 5.83 (m, 1 H,  $C_5H_3$ ), 6.14 (m, 1 H,  $C_5H_3$ ), 6.83 (m, 1 H,  $C_5H_3$ ), 6.87–7.20 (m, 10 H,  $CH_2Ph$ ) ppm.  $^{13}C$  NMR ( $C_6D_6$ , 20 °C):  $\delta = 0.6$  (SiMe<sub>2</sub>), 1.5 (SiMe<sub>2</sub>), 2.4 (SiMe<sub>2</sub>), 2.9 (SiMe<sub>2</sub>), 33.8 (NH<sub>t</sub>Bu), 34.2 (NtBu), 49.8 (NH<sub>t</sub>Bu<sub>tert</sub>), 61.5 (NtBu<sub>tert</sub>), 79.6 ( $CH_2Ph$ ), 83.7 ( $CH_2Ph$ ), 110.2 ( $C_5H_3$ ), 122.1 ( $C_5H_3$ ), 122.5 ( $C_5H_3$ ), 122.8 ( $C_5H_3$ ), 123.0 ( $C_5H_3$ ), 125.9 ( $C_6H_5$ ), 126.8 ( $C_6H_5$ ), 127.4 ( $C_6H_5$ ), 128.5 ( $C_6H_5$ ), 128.6 ( $C_6H_5$ ), 128.7 ( $C_6H_5$ ), 128.9 ( $C_6H_5$ ), 129.8 ( $C_6H_5$ ), 132.6 ( $C_6H_5$ ), 149.6 ( $C_6H_5$ ), 150.1 ( $C_6H_5$ ) ppm. IR (nujol):  $\tilde{\nu} = 3349$  (N–H) cm<sup>-1</sup>.  $C_{31}H_{48}N_2Si_2Ti$  (552.78): calcd. C 67.36, H 8.75, N 5.07; found C 67.82, H 8.71, N 4.81.

**[Zr{ $\eta^5$ -C<sub>5</sub>H<sub>3</sub>-1-[SiMe<sub>2</sub>(NH<sub>t</sub>Bu)]-3-[SiMe<sub>2</sub>( $\eta^1$ -NtBu)}](CH<sub>2</sub>Ph)<sub>2</sub>** (**7**): A solution of  $Zr(CH_2Ph)_4$  (2.93 g, 6.43 mmol) in toluene (70 mL) was cooled to 0 °C, and **1** (2.09 g, 6.43 mmol) was added by syringe. The resulting yellow solution was warmed to 40 °C for 5 h. The solvent was removed under vacuum and the residue was extracted into pentane (70 mL). After filtration and removal of the solvent, a mixture of complexes **7** and **11** was isolated. Formation of **7** was confirmed by IR and NMR spectroscopy, although pure **7** free of **11** could not be isolated. Data for **7**: IR (Nujol):  $\tilde{\nu} = 3353$  (N–H) cm<sup>-1</sup>.  $^1H$  NMR ( $C_6D_6$ , 20 °C):  $\delta = 0.33$  (s, 3 H, SiMe<sub>2</sub>NH<sub>t</sub>Bu), 0.34 (s, 3 H, SiMe<sub>2</sub>NH<sub>t</sub>Bu), 0.35 (s, 3 H, SiMe<sub>2</sub>NtBu), 0.40 (s, 3 H, SiMe<sub>2</sub>NtBu), 0.69 (s, 1 H, NH<sub>t</sub>Bu), 1.06

(s, 9 H, NH*t*Bu), 1.13 (s, 9 H, N*t*Bu), 1.66 (s, 1 H, CH<sub>2</sub>Ph), 1.72 (s, 1 H, CH<sub>2</sub>Ph), 2.12 (s, 1 H, CH<sub>2</sub>Ph), 2.17 (s, 1 H, CH<sub>2</sub>Ph), 6.21 (m, 1 H, C<sub>5</sub>H<sub>3</sub>), 6.35 (m, 1 H, C<sub>5</sub>H<sub>3</sub>), 6.60 (m, 1 H, C<sub>5</sub>H<sub>3</sub>), 6.90–7.30 (m, 10 H, C<sub>6</sub>H<sub>5</sub>) ppm. <sup>13</sup>C NMR (C<sub>6</sub>D<sub>6</sub>, 20 °C): δ = 1.3 (SiMe<sub>2</sub>), 2.0 (SiMe<sub>2</sub>), 2.4 (SiMe<sub>2</sub>), 2.5 (SiMe<sub>2</sub>), 33.7 (NH*t*Bu), 33.8 (N*t*Bu), 49.7 (NH*t*Bu<sub>tert</sub>), 54.9 (CH<sub>2</sub>Ph), 57.5 (N*t*Bu<sub>tert</sub>), 57.9 (CH<sub>2</sub>Ph), 109.6 (C<sub>5</sub>H<sub>3</sub>*ipso*), 122.2 (C<sub>5</sub>H<sub>3</sub>), 122.5 (C<sub>5</sub>H<sub>3</sub>), 124.8 (C<sub>5</sub>H<sub>3</sub>), 125.6 (C<sub>5</sub>H<sub>3</sub>), 125.9 (C<sub>6</sub>H<sub>5</sub>), 126.4 (C<sub>6</sub>H<sub>5</sub>), 126.6 (C<sub>6</sub>H<sub>5</sub>), 127.8 (C<sub>6</sub>H<sub>5</sub>), 129.3 (C<sub>6</sub>H<sub>5</sub>), 129.6 (C<sub>6</sub>H<sub>5</sub>), 129.6 (C<sub>6</sub>H<sub>5</sub>), 129.8 (C<sub>6</sub>H<sub>5</sub>), 131.9 (C<sub>6</sub>H<sub>5</sub>), 145.8 (C<sub>6</sub>H<sub>3</sub>*ipso*), 146.2 (C<sub>6</sub>H<sub>3</sub>*ipso*) ppm.

[Ti{η<sup>5</sup>-C<sub>5</sub>H<sub>3</sub>-1,3-[SiMe<sub>2</sub>(η<sup>1</sup>-N*t*Bu)]<sub>2</sub>} (NMe<sub>2</sub>)] (8): When a C<sub>6</sub>D<sub>6</sub> solution of the diamido complex **4** was heated at 160 °C for 12 h in a sealed NMR tube, a slow reaction took place with elimination of NHMe<sub>2</sub> to give **8**, identified by its <sup>1</sup>H and <sup>13</sup>C NMR spectra, together with the starting complex **4**. When the reaction mixture was cooled to room temperature, the reaction proved to be irreversible. <sup>1</sup>H NMR (C<sub>6</sub>D<sub>6</sub>, 20 °C): δ = 0.50 (s, 6 H, SiMe<sub>2</sub>), 0.52 (s, 6 H, SiMe<sub>2</sub>), 1.38 (s, 18 H, N*t*Bu), 2.83 (s, 6 H, NMe<sub>2</sub>), 6.17 (d, 2 H, C<sub>5</sub>H<sub>3</sub>), 6.71 (t, 1 H, C<sub>5</sub>H<sub>3</sub>) ppm. <sup>13</sup>C NMR (C<sub>6</sub>D<sub>6</sub>, 20 °C): δ = 2.7 (SiMe<sub>2</sub>), 2.8 (SiMe<sub>2</sub>), 35.2 (N*t*Bu), 51.3 (NMe<sub>2</sub>), 59.3 (N*t*Bu<sub>tert</sub>), 117.7 (C<sub>5</sub>H<sub>3</sub>*ipso*), 121.3 (C<sub>5</sub>H<sub>3</sub>), 131.9 (C<sub>5</sub>H<sub>3</sub>) ppm.

[Zr{η<sup>5</sup>-C<sub>5</sub>H<sub>3</sub>-1,3-[SiMe<sub>2</sub>(η<sup>1</sup>-N*t*Bu)]<sub>2</sub>} (NMe<sub>2</sub>)] (9). Method A: When a C<sub>6</sub>D<sub>6</sub> solution of the diamido complex **5** was heated at 120 °C for 12 h in a sealed NMR tube, a slow reaction took place with elimination of NHMe<sub>2</sub> to give **9**, identified by its <sup>1</sup>H and <sup>13</sup>C NMR spectra. However, when the reaction mixture was cooled to room temperature, a reversible reaction with the free NHMe<sub>2</sub> present in solution once more yielded the starting complex **5**. Method B: A 1:1 molar ratio of the benzyl derivative **11** (1.46 g, 3.1 mmol) and the diamido derivative **5** (1.45 g, 3.1 mmol) in toluene was heated at 120 °C in a Teflon-valved Schlenk tube for 12 h. The solvent was removed under vacuum and the residue was extracted into pentane (50 mL). After filtration and removal of the solvent, complex **9** (1.32 g, 2.9 mmol, 94%) was isolated as a yellow solid. <sup>1</sup>H NMR (C<sub>6</sub>D<sub>6</sub>, 20 °C): δ = 0.51 (s, 6 H, SiMe<sub>2</sub>), 0.55 (s, 6 H, SiMe<sub>2</sub>), 1.31 (s, 18 H, N*t*Bu), 2.77 (s, 6 H, NMe<sub>2</sub>), 6.34 (d, 2 H, C<sub>5</sub>H<sub>3</sub>), 6.78 (t, 1 H, C<sub>5</sub>H<sub>3</sub>) ppm. <sup>13</sup>C NMR (C<sub>6</sub>D<sub>6</sub>, 20 °C): δ = 2.9 (SiMe<sub>2</sub>), 3.0 (SiMe<sub>2</sub>), 35.6 (N*t*Bu), 45.1 (NMe<sub>2</sub>), 55.8 (N*t*Bu<sub>tert</sub>), 117.7 (C<sub>5</sub>H<sub>3</sub>*ipso*), 119.8 (C<sub>5</sub>H<sub>3</sub>), 133.2 (C<sub>5</sub>H<sub>3</sub>) ppm. C<sub>19</sub>H<sub>39</sub>N<sub>3</sub>Si<sub>2</sub>Zr (456.93): calcd. C 49.94, H 8.60, N 9.20; found C 50.28, H 8.31, N 8.86.

[Ti{η<sup>5</sup>-C<sub>5</sub>H<sub>3</sub>-1,3-[SiMe<sub>2</sub>(η<sup>1</sup>-N*t*Bu)]<sub>2</sub>} (CH<sub>2</sub>Ph)] (10): A solution of Ti(CH<sub>2</sub>Ph)<sub>4</sub> (5.34 g, 12.9 mmol) in toluene (70 mL) was cooled to 0 °C, and **1** (4.21 g, 12.9 mmol) was added by syringe. The resulting deep red solution was warmed at 70 °C for 5 h. The solvent was removed under vacuum and the residue was extracted into pentane (70 mL). After filtration and removal of the solvent, complex **10** was isolated as a waxy, red solid, which was recrystallized from hexane to give orange crystals (5.88 g, 12.7 mmol, 98%). <sup>1</sup>H NMR (C<sub>6</sub>D<sub>6</sub>, 20 °C): δ = 0.39 (s, 6 H, SiMe<sub>2</sub>), 0.40 (s, 6 H, SiMe<sub>2</sub>), 1.42 (s, 18 H, N*t*Bu), 2.59 (s, 2 H, CH<sub>2</sub>Ph), 6.12 (d, 2 H, C<sub>5</sub>H<sub>3</sub>), 6.39 (t, 1 H, C<sub>5</sub>H<sub>3</sub>), 6.89 (m, 1 H, C<sub>6</sub>H<sub>5</sub>), 6.95 (m, 2 H, C<sub>6</sub>H<sub>5</sub>), 7.22 (m, 2 H, C<sub>6</sub>H<sub>5</sub>) ppm. <sup>13</sup>C NMR (C<sub>6</sub>D<sub>6</sub>, 20 °C): δ = 2.1 (SiMe<sub>2</sub>), 2.2 (SiMe<sub>2</sub>), 35.6 (N*t*Bu), 59.3 (N*t*Bu<sub>tert</sub>), 69.6 (CH<sub>2</sub>Ph), 117.7 (C<sub>5</sub>H<sub>3</sub>*ipso*), 121.5 (C<sub>5</sub>H<sub>3</sub>), 126.3 (C<sub>5</sub>H<sub>3</sub>), 128.5 (C<sub>6</sub>H<sub>5</sub>), 130.3 (C<sub>6</sub>H<sub>5</sub>), 132.6 (C<sub>6</sub>H<sub>5</sub>), 152.4 (C<sub>6</sub>H<sub>3</sub>*ipso*) ppm. C<sub>24</sub>H<sub>40</sub>N<sub>2</sub>Si<sub>2</sub>Ti (460.63): calcd. C 62.58, H 8.75, N 6.08; found C 62.68, H 8.68, N 5.76.

[Zr{η<sup>5</sup>-C<sub>5</sub>H<sub>3</sub>-1,3-[SiMe<sub>2</sub>(η<sup>1</sup>-N*t*Bu)]<sub>2</sub>} (CH<sub>2</sub>Ph)] (11): A solution of Zr(CH<sub>2</sub>Ph)<sub>4</sub> (2.93 g, 6.43 mmol) in toluene (70 mL) was cooled to 0 °C, and **1** (2.09 g, 6.43 mmol) was added by syringe. The resulting yellow solution was heated at reflux for 5 h. The solvent was removed under vacuum and the residue was extracted into pentane

(70 mL). After filtration and removal of the solvent, complex **11** was isolated as a brown solid (3.20 g, 6.34 mmol, 99%). <sup>1</sup>H NMR (C<sub>6</sub>D<sub>6</sub>, 20 °C): δ = 0.40 (s, 6 H, SiMe<sub>2</sub>), 0.42 (s, 6 H, SiMe<sub>2</sub>), 1.27 (s, 18 H, N*t*Bu), 2.12 (s, 2 H, CH<sub>2</sub>Ph), 6.14 (d, 2 H, C<sub>5</sub>H<sub>3</sub>), 6.53 (t, 1 H, C<sub>5</sub>H<sub>3</sub>), 6.9–7.23 (m, 5 H, C<sub>6</sub>H<sub>5</sub>) ppm. <sup>13</sup>C NMR (C<sub>6</sub>D<sub>6</sub>, 20 °C): δ = 2.4 (SiMe<sub>2</sub>), 2.4 (SiMe<sub>2</sub>), 35.8 (N*t*Bu), 55.8 (CH<sub>2</sub>Ph), 57.1 (N*t*Bu<sub>tert</sub>), 116.5 (C<sub>5</sub>H<sub>3</sub>*ipso*), 120.7 (C<sub>5</sub>H<sub>3</sub>), 126.4 (C<sub>5</sub>H<sub>3</sub>), 128.5 (C<sub>6</sub>H<sub>5</sub>), 129.8 (C<sub>6</sub>H<sub>5</sub>), 132.7 (C<sub>6</sub>H<sub>5</sub>), 150.6 (C<sub>6</sub>H<sub>3</sub>*ipso*) ppm. C<sub>24</sub>H<sub>40</sub>N<sub>2</sub>Si<sub>2</sub>Zr (503.97): calcd. C 57.20, H 8.00, N 5.56; found C 57.01, H 7.65, N 5.48.

[Ti{η<sup>5</sup>-C<sub>5</sub>H<sub>3</sub>-1,3-[SiMe<sub>2</sub>(η<sup>1</sup>-N*t*Bu)]<sub>2</sub>} (12): A toluene (20 mL) solution of the monobenzyl complex **10** (0.125 g, 0.25 mmol) was treated at room temperature with B(C<sub>6</sub>F<sub>5</sub>)<sub>3</sub> (0.126 g, 0.25 mmol), and the mixture was stirred for 30 min and cooled to –35 °C. The solvent was filtered off from the resulting insoluble residue, which was then dried under vacuum to give **12** (0.13 g, 60% yield) as an orange, crystalline solid. <sup>1</sup>H NMR (C<sub>6</sub>D<sub>6</sub>, 20 °C): δ = 0.19 (s, 6 H, SiMe<sub>2</sub>), 0.38 (s, 6 H, SiMe<sub>2</sub>), 1.12 (s, 18 H, N*t*Bu), 3.49 (s, 2 H, BCH<sub>2</sub>), 5.03 (d, 2 H, C<sub>5</sub>H<sub>3</sub>), 5.86 (t, 1 H, C<sub>5</sub>H<sub>3</sub>), 6.21–7.10 (m, 5 H, C<sub>6</sub>H<sub>5</sub>) ppm. <sup>13</sup>C NMR (C<sub>6</sub>D<sub>6</sub>, 20 °C): δ = 0.6 (SiMe<sub>2</sub>), 1.4 (SiMe<sub>2</sub>), 34.6 (N*t*Bu), 59.3 (N*t*Bu<sub>tert</sub>), 122.1 (C<sub>5</sub>H<sub>3</sub>*ipso*), 126.1 (C<sub>5</sub>H<sub>3</sub>), 126.2 (C<sub>5</sub>H<sub>3</sub>), 128.3 (C<sub>6</sub>H<sub>5</sub>), 128.7 (C<sub>6</sub>H<sub>5</sub>), 132.9 (C<sub>6</sub>H<sub>5</sub>), 135.1 (C<sub>6</sub>F<sub>5</sub>), 140.1 (C<sub>6</sub>F<sub>5</sub>), 145.8 (C<sub>6</sub>F<sub>5</sub>), 150.9 (C<sub>6</sub>F<sub>5</sub>) ppm. <sup>19</sup>F NMR (300 MHz, C<sub>6</sub>D<sub>6</sub>, 20 °C, CCl<sub>3</sub>F): δ = 132.1 (m, 2 F, o-C<sub>6</sub>F<sub>5</sub>), 163.7 (m, 1 F, p-C<sub>6</sub>F<sub>5</sub>), 167.3 (m, 2 F, m-C<sub>6</sub>F<sub>5</sub>) ppm. C<sub>42</sub>H<sub>40</sub>BF<sub>15</sub>N<sub>2</sub>Si<sub>2</sub>Ti (972.63): calcd. C 51.87, H 4.15, N 2.88; found C 51.98, H 4.04, N 3.08.

[Zr{η<sup>5</sup>-C<sub>5</sub>H<sub>3</sub>-1,3-[SiMe<sub>2</sub>(η<sup>1</sup>-N*t*Bu)]<sub>2</sub>} (13): A toluene (20 mL) solution of the monobenzyl complex **11** (0.116 g, 0.25 mmol) was treated with B(C<sub>6</sub>F<sub>5</sub>)<sub>3</sub> (0.126 g, 0.25 mmol) at room temperature and the mixture was stirred for 30 min and cooled to –35 °C. The solvent was filtered off from the resulting insoluble residue, which was then dried under vacuum to give **13** (0.21 g, 83% yield) as a dark brown oil. After recrystallization, a suitable orange monocrystal of **13** was separated for X-ray diffraction studies. <sup>1</sup>H NMR (C<sub>6</sub>D<sub>6</sub>, 20 °C): δ = 0.17 (s, 6 H, SiMe<sub>2</sub>), 0.36 (s, 6 H, SiMe<sub>2</sub>), 0.99 (s, 18 H, N*t*Bu), 3.42 (s, 2 H, BCH<sub>2</sub>), 5.20 (d, 2 H, C<sub>5</sub>H<sub>3</sub>), 6.01 (t, 1 H, C<sub>5</sub>H<sub>3</sub>), 6.10 (m, 1 H, p-C<sub>6</sub>H<sub>5</sub>), 6.34 (m, 2 H, m-C<sub>6</sub>H<sub>5</sub>), 6.87 (m, 2 H, o-C<sub>6</sub>H<sub>5</sub>) ppm. <sup>13</sup>C NMR (C<sub>6</sub>D<sub>6</sub>, 20 °C): δ = 1.5 (SiMe<sub>2</sub>), 1.6 (SiMe<sub>2</sub>), 34.8 (N*t*Bu), 58.6 (N*t*Bu<sub>tert</sub>), 121.4 (C<sub>5</sub>H<sub>3</sub>), 123.5 (C<sub>5</sub>H<sub>3</sub>*ipso*), 127.4 (C<sub>5</sub>H<sub>3</sub>), 127.9 (C<sub>6</sub>H<sub>5</sub>), 128.1 (C<sub>6</sub>H<sub>5</sub>), 128.3 (C<sub>6</sub>H<sub>5</sub>), 136.5 (C<sub>6</sub>F<sub>5</sub>), 138.3 (C<sub>6</sub>F<sub>5</sub>), 147.8 (C<sub>6</sub>F<sub>5</sub>), 149.8 (C<sub>6</sub>F<sub>5</sub>), 162.0 (C<sub>6</sub>H<sub>3</sub>*ipso*) ppm. <sup>19</sup>F NMR (300 MHz, C<sub>6</sub>D<sub>6</sub>, 20 °C, CCl<sub>3</sub>F): δ = 132.1 (m, 2 F, o-C<sub>6</sub>F<sub>5</sub>), 163.6 (m, 1 F, p-C<sub>6</sub>F<sub>5</sub>), 167.2 (m, 2 F, m-C<sub>6</sub>F<sub>5</sub>) ppm. C<sub>42</sub>H<sub>40</sub>BF<sub>15</sub>N<sub>2</sub>Si<sub>2</sub>Zr (1015.97): calcd. C 49.65, H 3.97, N 2.76; found C 50.51, H 3.71, N 3.35.

**Crystal Structure Determination for Compound 10:** Crystals of **10** were grown from a hexane solution. An orange fragment in perfluorinated ether was selected and transferred to a glass capillary, which was mounted in a cold N<sub>2</sub> stream. Preliminary examination and data collection were carried out with a Nonius KappaCCD device at the window of a rotating anode X-ray generator with use of graphite-monochromated Mo-*K*<sub>α</sub> radiation ( $\lambda = 0.71073 \text{ \AA}$ ), controlled by the Collect software package.<sup>[25]</sup> Collected images were processed by use of Denzo. The unit cell parameters were obtained by full-matrix, least-squares refinements of 4895 reflections.<sup>[26]</sup> A total number of 41477 reflections were integrated. After merging, 4739 reflections remained, and these were used for all further calculations. Absorption effects were corrected during the scaling procedure. The structure was solved by direct methods<sup>[27]</sup> and refined by standard difference Fourier techniques.<sup>[28]</sup> All non-hydrogen atoms of the asymmetric unit were refined with aniso-

tropic thermal displacement parameters. All hydrogen atoms were found in the difference Fourier map and refined freely with individual isotropic thermal displacement parameters, except for those located at a disordered *tert*-butyl group, which were placed in calculated positions (riding model). Full-matrix, least-squares refinements were carried out by minimization of  $\Sigma w(F_o^2 - F_c^2)^2$  by use of the SHELXL-97 weighting scheme and stopped at a maximum shift/err < 0.001.<sup>[28,29,30]</sup> One *tert*-butyl group in **10** appears to be disordered over two positions (73:27).

**Crystal Structure Determination for Compound 13:** Crystals of **13** were grown from a C<sub>6</sub>D<sub>6</sub> solution. An orange plate in perfluorinated ether was selected and transferred to a glass capillary. Preliminary examination and data collection were carried out with a Nonius KappaCCD device at the window of a rotating anode X-ray generator by use of graphite-monochromated Mo-K<sub>α</sub> radiation ( $\lambda = 0.71073 \text{ \AA}$ ), controlled by the Collect software package.<sup>[26]</sup> Collected images were processed by use of Denzo. The unit cell parameters were obtained by full-matrix, least-squares refinements of 8080 reflections.<sup>[27]</sup> A total number of 44162 reflections were integrated. After merging, 8099 reflections remained and were used for all further calculations. Absorption effects were corrected during the scaling procedure. The structure was solved by direct methods<sup>[27]</sup> and refined by standard difference Fourier techniques.<sup>[28]</sup> All non-hydrogen atoms of the asymmetric unit were refined with anisotropic thermal displacement parameters. All hydrogen atoms were found in the difference Fourier map and refined freely with individual isotropic thermal displacement parameters. Full-matrix, least-squares refinements were carried out by minimization of  $\Sigma w(F_o^2 - F_c^2)^2$  by use of the SHELXL-97 weighting scheme and stopped at a maximum shift/err < 0.001. A correction for extinction effects was applied.<sup>[28–30]</sup>

CCDC-200139 (**10**) and -200140 (**13**) contain the supplementary crystallographic data for this paper. These data can be obtained free of charge at [www.ccdc.cam.ac.uk/conts/retrieving.html](http://www.ccdc.cam.ac.uk/conts/retrieving.html) [or from the Cambridge Crystallographic Data Centre, 12 Union Road, Cambridge CB2 1EZ, UK; Fax: (internat.) + 44-1223/336-033; E-mail: deposit@ccdc.cam.ac.uk].

**Computational Details:** Gradient corrected density functional calculations were carried out, with corrections for exchange and correlation according to Becke<sup>[31]</sup> and Perdew,<sup>[32]</sup> respectively (BP86). Geometries were optimized by use of the TURBOMOLE<sup>[33]</sup> program system within the framework of the RI-J approximation.<sup>[34]</sup> For the model systems, a triple- $\zeta$  valence basis plus polarization TZVP<sup>[35]</sup> was employed. For the geometry optimization of the real molecules, the main group elements were described by a split-valence basis set<sup>[36]</sup> with one set of polarization functions for the non-H atoms, and Ti was treated with the TZVP basis. For the determination of bond energies, final energies were obtained in a single-point calculation using the TZVP basis set for all atoms.

## Acknowledgments

The authors acknowledge the MCyT (project MAT2001-1309) for financial support and the EC (project COST-D12/0016/98). J. C. acknowledges CAM for a fellowship.

[1] [1a] P. C. Möhring, N. J. Coville, *J. Organomet. Chem.* **1994**, *479*, 1–29. [1b] H. H. Brintzinger, D. Fischer, R. Mülhaupt, B. Rieger, R. M. Waymouth, *Angew. Chem. Int. Ed. Engl.* **1995**, *34*, 1143–1170. [1c] G. G. Hlatky, *Coord. Chem. Rev.* **1999**, *181*, 243–296. [1d] H. G. Alt, A. Köppel, *Chem. Rev.* **2000**, *100*, 1205–1222. [1e] L. Resconi, L. Cavallo, A. Fait, F. Piemontesi, *Chem. Rev.* **2000**, *100*, 1253–1345.

Table 4. Crystallographic data for complexes **10** and **13**

	<b>10</b>	<b>13</b>
Empirical formula	C <sub>24</sub> H <sub>40</sub> N <sub>2</sub> Si <sub>2</sub> Ti	C <sub>42</sub> H <sub>40</sub> BF <sub>15</sub> N <sub>2</sub> Si <sub>2</sub> Zr
Formula mass	460.63	1015.97
Colour/shape	orange/fragment	orange/plate
Crystal size [mm]	0.36 × 0.23 × 0.20	0.56 × 0.30 × 0.10
Crystal system	monoclinic	triclinic
Space group	P2 <sub>1</sub> /c (No. 14)	P\bar{1} (No. 2)
<i>a</i> [\text{\AA}]	10.6962(1)	11.7349(1)
<i>b</i> [\text{\AA}]	16.0412(2)	13.4253(1)
<i>c</i> [\text{\AA}]	15.3339(2)	14.4024(1)
$\alpha$ [ $^\circ$ ]	90	77.4374(3)
$\beta$ [ $^\circ$ ]	99.6928(7)	88.2620(4)
$\gamma$ [ $^\circ$ ]	90	86.9316(5)
<i>V</i> [\text{\AA}³]	2593.43(5)	2211.12(3)
<i>Z</i>	4	2
<i>T</i> [K]	123	293
$\rho_{\text{calcd.}}$ [g cm <sup>-3</sup> ]	1.180	1.526
$\mu$ [mm <sup>-1</sup> ]	0.435	0.399
<i>F</i> <sub>000</sub>	992	1028
$\theta$ range [ $^\circ$ ]	1.85–25.34	1.45–25.38
Data collected ( <i>h,k,l</i> )	$\pm 12, \pm 19, \pm 18$	$\pm 14, \pm 16, \pm 17$
No. of reflns. collected	41477	44162
No. of independent reflns./ <i>R</i> <sub>int</sub>	4739 (all)/0.033	8099 (all)/0.033
No. of obsd. reflns. ( <i>I</i> > 2 <i>σ</i> ( <i>I</i> ))	4193 (obsd.)	7177 (obsd.)
No. of params. refined	414	729
<i>R</i> 1 (obsd./all)	0.0333/0.0394	0.0306/0.0370
<i>wR</i> 2 (obsd./all)	0.0855/0.0895	0.0752/0.0788
GOF (obsd./all)	1.045/1.045	1.040/1.040
max./min. $\Delta\rho$ [e·Å <sup>-3</sup> ]	+0.32/−0.27	+0.30/−0.27

- [2] [2a] P. J. Shapiro, E. E. Bunel, W. E. Piers, J. E. Bercaw, *Synlett* **1990**, *2*, 74–84. [2b] P. J. Shapiro, E. Bunel, W. P. Schäfer, J. E. Bercaw, *Organometallics* **1990**, *9*, 867–869. [2c] P. J. Shapiro, W. E. Cotter, W. P. Schäfer, J. A. Labinger, J. E. Bercaw, *J. Am. Chem. Soc.* **1994**, *116*, 4623–4640. [2d] J. Okuda, *Chem. Ber.* **1990**, *123*, 1649–1651. [2e] A. K. Hughes, A. Meetsma, J. H. Teuben, *Organometallics* **1993**, *12*, 1936–1945. [2f] W. A. Herrmann, M. J. A. Morawietz, *J. Organomet. Chem.* **1994**, *482*, 169–181. [2g] S. Ciruelos, T. Cuénca, R. Gómez, P. Gómez-Sal, A. Manzanero, P. Royo, *Organometallics* **1996**, *15*, 5577–5585. [2h] R. Gómez, P. Gómez-Sal, A. Martín, A. Núñez, P. A. del Real, P. Royo, *J. Organomet. Chem.* **1998**, *564*, 93–100. [2i] A. L. McKnight, R. M. Waymouth, *Chem. Rev.* **1998**, *98*, 2587–2598. [2j] J. Klosin, W. J. Kruper, Jr., P. N. Nickias, G. R. Roof, P. DeWaele, K. A. Abboud, *Organometallics* **2001**, *20*, 2663–2665. [2k] K. Kunz, G. Erker, S. Döring, R. Fröhlich, G. Kehr, *J. Am. Chem. Soc.* **2001**, *123*, 6181–6182. [3] [3a] M. Bochmann, *J. Chem. Soc., Dalton Trans.* **1996**, 255–270. [3b] C. P. Casey, D. W. Carpenetti II, H. Sakurai, *Organometallics* **2001**, *20*, 4262–4265. [3c] C. G. Brandow, A. Mendiratta, J. E. Bercaw, *Organometallics* **2001**, *20*, 42534261. [4] [4a] Y.-X. Chen, P.-F. Fu, C. L. Stern, T. J. Marks, *Organometallics* **1997**, *16*, 5958–5963. [4b] B. E. Bosch, G. Erker, R. Fröhlich, O. Meyer, *Organometallics* **1997**, *16*, 5449–5456. [4c] Y.-X. Chen, T. J. Marks, *Organometallics* **1997**, *16*, 3649–3657. [4d] A. Bertuleit, C. Fritze, G. Erker, R. Fröhlich, *Organometallics* **1997**, *16*, 2891–2899. [4e] G. Lanza, I. L. Fragalà, T. J. Marks, *J. Am. Chem. Soc.* **1998**, *120*, 8257–8258. [4f] F. Amor, A. Butt, K. E. Du Plooy, T. B. Spaniol, J. Okuda, *Organometallics* **1998**, *17*, 5836–5849. [4g] R. Gómez, P. Gómez-Sal, P. A. del Real, P. Royo, *J. Organomet. Chem.* **1999**, *588*, 22–27. [4h] R. J. Keaton, K. C. Jayaratne, J. C. Fettinger, L. R. Sita, *J. Am. Chem. Soc.* **2000**, *122*, 12909–12910. [4i] J.-F. Carpentier, V. P.

- Maryin, J. Luci, R. F. Jordan, *J. Am. Chem. Soc.* **2001**, *123*, 898–909.
- [5] [5a] J. C. Stevens, F. J. Timmers, D. R. Wilson, G. F. Schmidt, P. N. Nickias, R. K. Rosen, G. W. Knight, S. Y. Lai, *Eur. Patent Appl. EP* **1991**, 416815 (Dow Chemical Co.) (*Chem. Abstr.* **1991**, *115*, 93163). [5b] J. M. Canich, *Eur. Patent Appl. EP* **1991**, 420436 (Exxon Chemical Co) (*Chem. Abstr.* **1991**, *115*, 184145).
- [6] V. C. Gibson, *J. Chem. Soc., Dalton Trans.* **1994**, 1607–1618.
- [7] [7a] J. Cano, P. Royo, A. Tiripicchio, M. A. Pellinghelli, M. Lanfranchi, *Angew. Chem. Int. Ed.* **2001**, *40*, 2495–2497. [7b] P. Royo, J. Cano, M. A. Flores, B. Peña, EP **2001**, 1225179 A1; US **2002**, 0115560 A1.
- [8] [8a] B. E. Bursten, L. F. Rhodes, J. Strittmatter, *J. Am. Chem. Soc.* **1989**, *111*, 2758–2766. [8b] T. Brackemeyer, G. Erker, R. Fröhlich, *Organometallics* **1997**, *16*, 531–536. [8c] H. Jacobsen, H. Berke, S. Doring, G. Kehr, G. Erker, R. Fröhlich, O. Meyer, *Organometallics* **1999**, *18*, 1724–1735. [8d] N. Kliegrewie, T. Brakemeyer, R. Fröhlich, G. Erker, *Organometallics* **2001**, *20*, 1952–1955.
- [9] J. M. Rozell, P. R. Jones, *Organometallics* **1985**, *4*, 2206–2210.
- [10] [10a] Y. A. Ustynyuk, A. V. Kisin, J. M. Pribytkova, A. A. Zarikin, N. D. Antonova, *J. Organomet. Chem.* **1972**, *42*, 47–63. [10b] P. Jutzi, *Chem. Rev.* **1986**, *86*, 983–996.
- [11] G. M. Diamond, R. F. Jordan, J. L. Petersen, *J. Am. Chem. Soc.* **1996**, *118*, 8024–8033.
- [12] U. Zucchini, E. Albizzati, U. Giannini, *J. Organomet. Chem.* **1971**, *26*, 357–372.
- [13] Y. Mu, W. E. Piers, L. R. MacQuarrie, M. Zaworotko, J. Young, *Organometallics* **1996**, *15*, 2720–2726.
- [14] D. M. P. Mingos, *Essential Trends in Inorganic Chemistry*, Oxford Univ. Press, Oxford, **1998**, p. 368.
- [15] [15a] W. A. Nugent, B. L. Haymore, *Coord. Chem. Rev.* **1980**, *31*, 123–175. [15b] D. E. Wigley, *Prog. Inorg. Chem.* **1994**, *42*, 239–482. [15c] M. J. Humphries, M. L. H. Green, M. A. Leech, V. C. Gibson, M. Jolly, D. N. Williams, M. R. J. Elsegood, W. Clegg, *J. Chem. Soc., Dalton Trans.* **2000**, 4044–4051.
- [16] J. Okuda, T. Eberle, T. P. Spaniol, *Chem. Ber./Recueil* **1997**, *130*, 209–215.
- [17] J. Okuda, S. Verch, R. Sturmer, T. P. Spaniol, *J. Organomet. Chem.* **2000**, *605*, 55–67.
- [18] A. Martín, M. Mena, C. Yelamos, R. Serrano, P. R. Raithby, *J. Organomet. Chem.* **1994**, *467*, 79–84.
- [19] D. W. Carpenetti, L. Kloppenburg, J. T. Kupec, J. L. Petersen, *Organometallics* **1996**, *15*, 1572–1581.
- [20] W. S. Seo, Y. J. Cho, S. C. Yoon, J. T. Park, Y. Park, *J. Organomet. Chem.* **2001**, *640*, 79–84.
- [21] Y. Mu, W. E. Piers, L. R. MacQuarrie, M. Zaworotko, *Can. J. Chem.* **1996**, *74*, 1696–1703.
- [22] J. Okuda, F. J. Schattenmann, S. Wocadlo, W. Massa, *Organometallics* **1995**, *14*, 789–795.
- [23] [23a] K. Shelly, D. C. Finster, Y. J. Lee, W. R. Scheidt, C. A. Reed, *J. Am. Chem. Soc.* **1985**, *107*, 5955–5959. [23b] M. Laguna, M. D. Villacampa, M. Contel, J. Garrido, *Inorg. Chem.* **1998**, *37*, 133–135. [23c] A. S. Batsanov, S. P. Crabtree, J. A. K. Howard, C. W. Lehmann, M. Kilner, *J. Organomet. Chem.* **1998**, *550*, 59–61.
- [24] A. G. Massey, A. J. Park, *J. Organomet. Chem.* **1964**, *2*, 245–250.
- [25] COLLECT, *Data Collection Software for Nonius Kappa CCD Devices*, Hooft, R. Nonius B. V., Delft, The Netherlands, **1998**.
- [26] Z. Otwinowski, W. Minor, *Processing of X-ray Diffraction Data Collected in Oscillation Mode, Methods in Enzymology*, vol. 276: *Macromolecular Crystallography*, part A (Eds.: C. W. Carter, Jr., R. M. Sweet), Academic Press, New York, **1997**, p. 307–326.
- [27] A. Altomare, G. Cascarano, C. Giacovazzo, A. Guagliardi, M. C. Burla, G. Polidori, M. Camalli, *J. Appl. Crystallogr.* **1994**, *27*, 435–436.
- [28] G. M. Sheldrick, *SHELXL-97*, Universität Göttingen, Germany **1998**.
- [29] International Tables for Crystallography, vol. C, Tables 6.1.1.4 (pp. 500–502), 4.2.6.8 (pp. 219–222), and 4.2.4.2 (pp. 193–199) (Ed.: A. J. C. Wilson), Kluwer Academic Publishers, Dordrecht, **1992**.
- [30] A. L. Spek, *Acta Crystallogr., Sect. A* **1990**, *46*, C34.
- [31] A. D. Becke, *Phys. Rev.* **1988**, *A38*, 3098–3100.
- [32] J. P. Perdew, *Phys. Rev.* **1986**, *B33*, 8822–8824.
- [33] [33a] R. Ahlrichs, M. Bär, M. Häser, H. Horn, C. Kölmel, *Chem. Phys. Lett.* **1989**, *162*, 165–169. [33b] O. Treutler, R. Ahlrichs, *J. Chem. Phys.* **1995**, *102*, 346–354. [33c] R. Ahlrichs, M. von Arnim, *Methods and Techniques in Computational Chemistry: METECC-95* (Eds.: E. Clementi, G. Corongiu), STEF, Cagliari, **1995**, chapter 13. [33d] R. Ahlrichs, M. von Arnim, *J. Comput. Chem.* **1998**, *19*, 1746–1757.
- [34] [34a] K. Eichkorn, O. Treutler, H. Öhm, M. Häser, R. Ahlrichs, *Chem. Phys. Lett.* **1995**, *242*, 652–660. [34b] K. Eichkorn, F. Weigand, O. Treutler, R. Ahlrichs, *Theor. Chem. Acc.* **1997**, *97*, 119–124.
- [35] A. Schäfer, C. Huber, R. Ahlrichs, *J. Chem. Phys.* **1994**, *100*, 5829–5835.
- [36] A. Schäfer, H. Horn, R. Ahlrichs, *J. Chem. Phys.* **1992**, *97*, 2571–2577.

Received December 20, 2002